6 Front-end limitations to infant spatial vision: Examination of two analyses

MARTIN S. BANKS AND JAMES A. CROWELL

After more than a decade of intense research, it is now widely recognized that visual sensitivity early in life is rather poor (Dobson and Teller, 1978; Banks and Salapatek, 1983; Brown, 1990). For example, contrast sensitivity and grating acuity during the first month of life are at least an order of magnitude worse than during adulthood. From birth to maturity the eye undergoes significant growth (Larsen, 1971), and the morphology of the photoreceptors, particularly the foveal cones, changes strikingly. Because these changes are extensive, it is natural to wonder to what extent optical and receptoral maturation causes the observed changes in visual sensitivity. The answer to this question is controversial; and, interestingly, the controversy stems primarily from differing assumptions about how age-related anatomical changes in the eye and retina ought to affect visual sensitivity rather than from disagreements about what those anatomical changes are. Specifically, Banks and Bennett (1988) and Wilson (1988) (see also Chapter 32) have used the same quantitative data on the growth of the eye and the photoreceptors to reach essentially opposite conclusions. Banks and Bennett concluded that age-related changes in eye size and foveal cone properties were not sufficient to account for the observed disparities between neonatal and adult contrast sensitivity and acuity, and Wilson concluded that they were nearly sufficient.

Obviously, the issue under debate is important to our understanding of visual development. If Wilson is right, the sometimes dramatic postnatal changes in retinal circuitry, lateral geniculate cell size and circuitry, and arborization of visual cortex have little measurable effect on our standard measures of visual sensitivity. In this chapter we examined the developmental analyses of Banks and Bennett and of Wilson more carefully and concluded that they actually lead to similar conclusions: In both cases, the authors showed that changes in eye size and foveal cone properties can account for much of the observed improvement in contrast sensitivity and grating acuity but are insufficient to explain all of it.

The chapter is organized as follows. First we describe the independent and combined effects of filtering and sampling that occurs in the front-end of the visual system; the experienced reader may wish to skim this section. Then we describe the Banks and Bennett (1988) analysis of the extent to which optical and receptoral immaturities limit early sensitivity. We next describe Wilson's (1988) (see also Chapter 32) developmental model, followed by a discussion and evaluation of the differences between the two analyses. We then modify Wilson's model by making more reasonable assumptions for some of the modeling parameters and examine the predictions of that model. Finally, we compare the predictions of the two approaches and discuss implications.

FILTERING AND SAMPLING BY THE OPTICS, RECEPTORS, AND NEURAL TRANSFER FUNCTION

Our analysis is based on the spatial contrast sensitivity function (CSF), which relates the inverse of the contrast required to detect a target to the target's spatial frequency; later we discuss the models' predictions of acuity. Signals entering the visual system are affected by the optics, the properties of the receptor lattice, the properties of individual receptors, and the postreceptoral processes. The models under consideration here assume that all these factors can be represented by linear filtering and sampling stages, so we can represent their effects in the following way:

$$g(x,y) = P^2 \cdot T \cdot E \cdot \{[i(x,y) * o(x,y) * r(x,y)] \cdot s(x,y)\} * n(x,y) \quad (1)$$

where $\cdot$ and $*$ = multiplication and convolution, respectively; i = the stimulus (specifically, its luminance function); g = the output of the sequence of processing stages; P = the numerical aperture of the eye (the pupil

diameter divided by the focal length)[1]; T = the transmittance of the ocular media (the proportion of incident photons that reach the retina); E = the efficiency of individual receptors in converting incident photons into isomerizations (specifically, the proportion of photons incident to the outer segments that are absorbed by the photopigment); $o(x, y)$ = the optical quality of the eye (i.e., the optical point-spread function); $r(x, y)$ = the aperture of individual receptors; $s(x, y)$ = the sampling function specifying the positions of receptors in the lattice; and $n(x, y)$ = the postreceptor transfer function. This equation can also be written in the spatial frequency domain as:

$$G(u, v) = P^2 \cdot T \cdot E \cdot \{[I(u, v) \cdot O(u, v) \cdot R(u, v)] * S(u, v)\} \cdot N(u, v) \quad (2)$$

where G, I, O, R, S, and N = the Fourier transforms of the functions represented by lower-case letters in Eq. (1); and u and v = horizontal and vertical spatial frequencies, respectively.

Before considering the Banks and Bennett and Wilson analyses, we examine the influence of each of these factors on contrast sensitivity in a manner that is mostly model-independent. Using optical, anatomical, densitometric, and psychophysical data in the literature, we can provide suitably accurate estimates of the transmission of the signal through the ocular media and formation into the retinal image and of the sampling and isomerizing properties of the receptor mosaic. We use these estimates to derive CSFs for two different assumptions about the shape of the neural transfer function (NTF), represented by $N(u, v)$. These two assumptions represent two simple models of the variation in receptive field size as a function of preferred spatial frequency.

Figure 6-1 represents the approach. Two stimuli—a grating (α) and a uniform field (β)—are presented and processed through the stages shown. Finally, a decision strategy is used to judge whether the grating or uniform field was presented on a given trial. The decision strategy used here is an ideal decision rule, that is, an optimal rule for discriminating α from β given the constraints imposed by the processing stages. We employ an ideal decision rule because it is the only rule that preserves all the discrimination information available (Geisler, 1984; Watson, 1985); in this way, we can examine the information losses that occur during the processing stages under consideration rather than during the decision process itself.

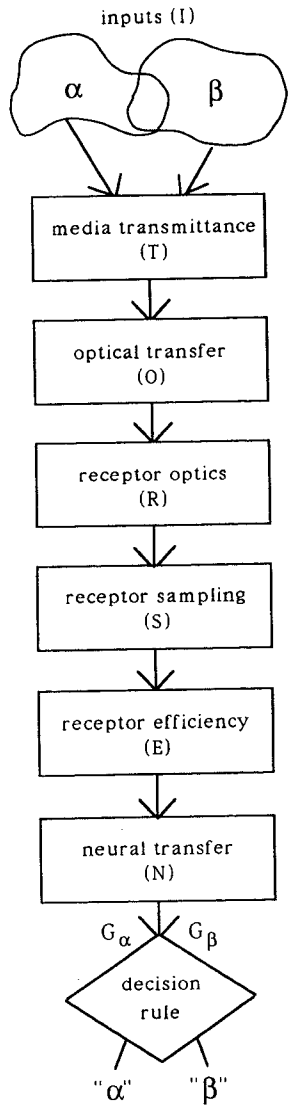

FIG. 6-1. Sequential ideal-observer analysis approach (Geisler, 1984). Two stimuli—a grating (α) and a uniform field (β)—are passed through the various processing stages shown here. At the end of the sequence, an ideal decision rule is used to determine the discriminability of the processed stimuli. We can determine the effect of the various stages on contrast sensitivity by making all stages but one perfect (or fixing them at some reasonable value) and varying the parameters of the stage of interest.

PUPIL, MEDIA TRANSMITTANCE, AND RECEPTOR EFFICIENCY

Three of the factors—the numerical aperture (P), the transmittance of the ocular media (T), and the efficiency of the photopigment-laden part of the receptors (E)—

1. Variations in pupil diameter have two effects on retinal image formation. First, it affects the proportion of photons incident to the eye that pass into the retinal image. This effect is represented by our value P. Second, the optical quality of the eye is affected by the diameter of the pupil too (Campbell and Gubisch, 1966); larger pupils are generally associated with poorer optical quality. This second effect is represented by $o(x, y)$, or in the frequency domain by $O(u, v)$, which represents the optical transfer function of the eye.

affect only the proportion of photons approaching the eye that are actually caught and produce signals; these effects are independent of the spatial frequency of the stimulus. Obviously, a change in the space-average luminance of the input stimuli has the same effect. Both approaches under consideration here—those of Banks and Bennett (1988) and of Wilson (1988) (see also Chapter 32)—assume that changes in photon catch affect contrast sensitivity according to square-root law (Rose, 1952; Barlow, 1958). Specifically, a K-fold increase in photon catch leads to a square root of K-fold increase in contrast sensitivity. Square-root law is a consequence of the Poisson probability distribution that describes the statistical properties of light. Incorporating this assumption in the models examined later is equivalent to assuming that contrast sensitivity is limited by quantal fluctuations in the stimulus. To show the effects of changes in P, T, E, or the space-average luminance of the stimulus, we have computed the contrast sensitivity of a system with perfect optics [$O(u, v)$], that is, optics that pass all spatial frequencies with equal fidelity), perfect receptor optics [$R(u, v)$] (all frequencies passed with equal fidelity through the receptors), and a flat neural transfer function [$N(u, v)$] (meaning that all frequencies are passed with equal strength through the postreceptoral circuits). In mathematical terms, we set the functions $O(u, v)$, $R(u, v)$, and $N(u, v)$ to constants so their effects on contrast sensitivity do not vary with spatial frequency. An ideal decision rule was used to compute the contrast sensitivity of such a system; the ideal decision rule, derived by Geisler (1984), consists in responding based on the value of the following decision variable (C):

$$C = \sum_{i=1}^{n} Z_i \ln(\alpha_i/\beta_i)$$

where Z_i = the observed photon catch at the ith receptor; and α_i and β_i = the expected catches at the ith receptor if either stimulus α or β was present. The ideal decision rule consists in constructing a weighting function $\ln(\alpha_i/\beta_i)$, which in the tasks we consider here is nearly equivalent to constructing a template of the expected grating target. In this chapter, we consider two-alternative, forced-choice experiments: The value of C is computed for each alternative, and the one with the higher value of C is assumed to have contained stimulus α. Other details of this system are provided in Table 6-1. Figure 6-2 shows the resulting CSFs. The parameter of the functions is the number of photons presented to the receptors per unit area per second. The upper function shows ideal contrast sensitivity when space-average luminance is 50 candelas per square meter (cd/m^2) and pupil diameter is 6 mm (retinal illuminance, the product of external luminance and pupil area, is 1413 trolands).

TABLE 6-1. *Values Used for Modeling*

Factor	Neonate	15 Month-old	Adult
Media transmittance (555 nm)	0.54	0.54	0.54
Pupil diameter (mm)	2.2	2.7	3.3
Posterior nodal distance (mm)	11.7	14.4	16.7
Receptor aperture (min)	0.35	0.67	0.48
Receptor spacing (min)	2.30	1.27	0.58
Outer segment length (μm)	3.1	22.5	50.0
Isomerization rate (555 nm)	0.05	0.28	0.50

The media was assumed to transmit 54% of the light (at 555 nm) incident on the cornea to the retina, and the photopigment was assumed to absorb 50% of the photons at 555 nm incident on receptors and other amounts at different wavelengths in correspondence with the L- and M-cone pigment sensitivities. The two lower functions show sensitivity when the retinal illuminance is reduced by 1 or 2 log units, which could be achieved (all other factors remaining constant) by reducing the external luminance by these values, reducing media transmittance by these values, or reducing the numerical aperture of the eye by the square root of these values. For each log unit of reduction in the number of incident photons, sensitivity falls by 0.5 log unit, thus obeying square-root law. Changes in receptor efficiency have the same effect.

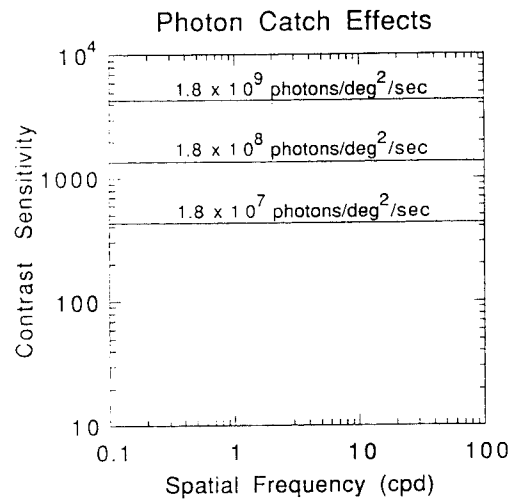

FIG. 6-2. Effect of photon catch on ideal contrast sensitivity. The three curves are ideal CSFs; the parameter of the functions is the number of photons presented to the receptors per unit area per second. The upper function shows ideal contrast sensitivity when retinal illuminance equals 1413 td, target duration is 250 ms, and large grating patches are presented. The two lower functions show sensitivity when either the retinal illuminance is reduced by 1 or 2 log units or the media transmittance is lowered by the same amounts. For each log unit of reduction in the number of incident photons, sensitivity falls by 0.5 log unit, thus obeying square-root law. Changes in receptor efficiency have the same effect.

OPTICS

Next we examine the influence of the optical quality of the eye. We do so by constructing a system in which the media transmittance and receptor efficiency are those of the mature fovea, and the receptor apertures and receptor spacing are set to small values so they do not affect the calculated sensitivities. The optical transfer functions (OTFs) used in this analysis are from Campbell and Gubisch (1966), who measured OTFs at different pupil diameters using the double-pass technique.[2] Again, an ideal decision rule is used to discriminate α and β based on the information available in G_α and G_β. Figure 6-3 shows the normalized contrast sensitivity of such a system limited by the optics. Optical transfer is poorer at larger pupil diameters. Note, for example, the spatial frequency at which transfer falls to 1% at different pupil diameters: 57, 50, 40, and 30 cycles per degree (cpd) at 2, 3, 3.8, and 5.8 mm, respectively.

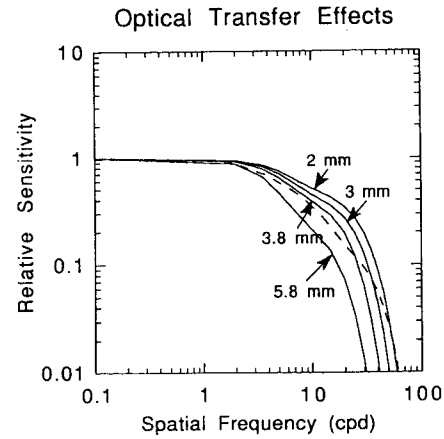

FIG. 6-3. OTFs for different pupil diameters. The solid curves are data from Campbell and Gubisch (1966) for pupil diameters of 2.0, 3.0, 3.8, and 5.8 mm; the dashed curve is M.S.B.'s OTF for a 4-mm pupil. Considering only the solid curves, it is clear that increasing pupil diameter has no effect at low frequencies but leads to greater and greater attenuation at high frequencies. This figure also demonstrates that M.S.B.'s optics are exceptionally good at high frequencies.

RECEPTOR APERTURE

To consider the influence of receptor optics on contrast sensitivity we again assume perfect optics and a flat neural transfer function and then vary the diameter of the receptor apertures. Other details of this system are given in Table 6-1. The receptor apertures are represented by cylinder functions of various diameters. Figure 6-4 plots the contrast sensitivities of this observer for different aperture diameters; the sensitivity of the system with an aperture of 0.48 minute has been set to 1 and the others plotted relative to that value. The plots are equivalent to the Fourier transforms of cylinder functions; that is, they are sombrero functions whose first zeroes occur at 1.22 times the reciprocals of the aperture diameters (Gaskill, 1978). The functions have small bumps at higher spatial frequencies, but in the interest of clarity they were suppressed in this figure.

Two effects are evident: (1) At small diameters, the CSF extends to high spatial frequencies, which makes intuitive sense: Receptors integrate light across their apertures, so large receptors are less able to signal fine detail in the image. (2) The low-frequency end of the CSF is higher for large receptor diameters. This finding also makes sense because an array of large receptors ought to collect more light than an array of small receptors with the same spacing. Banks and Bennett (1988) referred to the second effect as *retinal coverage*, arguing that the percentage of the retinal area covered by receptor apertures determines the proportion of incident photons that can be delivered to the photopigment.

2. Measuring the quality of an image reflected off the retina; the image passes through the optics twice.

RECEPTOR SPACING

To examine the influence of receptor spacing on contrast sensitivity we construct a system with perfect optics, a flat neural transfer function, and receptor apertures of 0.48 minute, the value assumed for the mature fovea. Again an ideal decision rule is employed. Other details are given in Table 6-1. Figure 6-5 displays CSFs for such a system with receptor spacing varying from

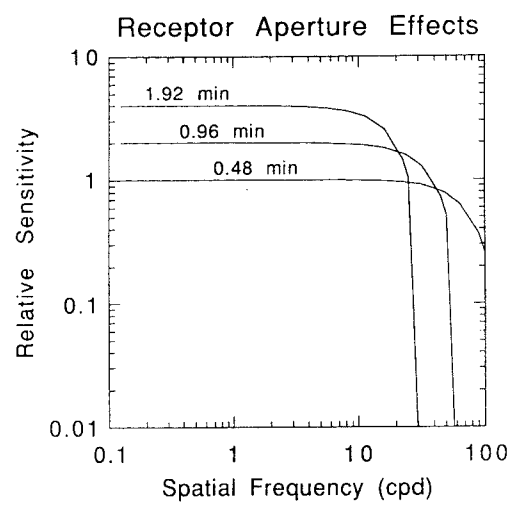

FIG. 6-4. Effect of receptor aperture size on ideal contrast sensitivity. The curves here are normalized CSFs for an ideal observer with perfect optics and a flat NTF and receptor apertures represented by cylinder functions of various sizes. Note that as the aperture size increases: (1) low-frequency sensitivity increases because the receptors are catching more photons; and (2) high-frequency sensitivity decreases because individual receptors are integrating over larger areas.

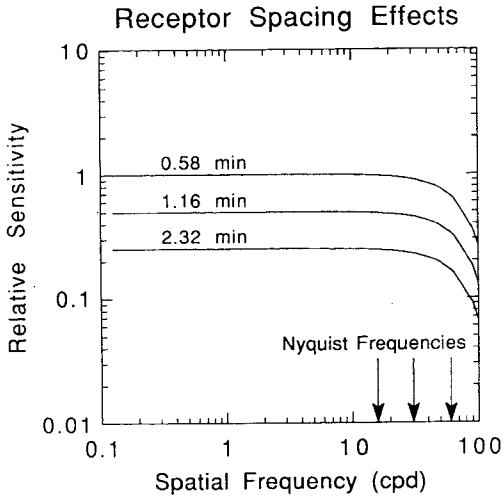

FIG. 6-5. Effect of receptor spacing on ideal contrast sensitivity. The ideal observer used to make this figure had perfect optics, a flat neural transfer function, and receptor apertures of 0.48 minute (Table 6-1). Receptors were arranged hexagonally. Note that (1) as receptor spacing increases from 0.58 to 2.32 minutes, sensitivity decreases; (2) this drop in sensitivity is independent of spatial frequency and in particular bears no relation to the Nyquist frequency. From left to right, the three arrows indicate the Nyquist frequencies for 2.32-, 1.16-, and 0.58-minute spacings, respectively.

0.58 minute (the value assumed for the mature fovea) to 2.32 minutes. There are two important points here. First, increases in receptor spacing lead to poorer contrast sensitivity, which makes sense because with receptors of fixed aperture size a lattice of widely spaced receptors catches fewer photons than one with finely spaced receptors. For every doubling of receptor spacing, the number of photons incident on receptor apertures decreases by a factor of 4; therefore, following square-root law, sensitivity decreases by a factor of 2. Second, the contrast sensitivity of the model system does not dip in the region of the Nyquist frequency, the highest spatial frequency a lattice can signal without distortion due to aliasing. The Nyquist frequencies are indicated by the arrows; the leftmost arrow is associated with a spacing of 2.32 minutes and the rightmost with a spacing of 0.58 minutes. The fact that contrast sensitivity does not dip near or above the Nyquist frequency might seem surprising at first, but recall that an ideal decision rule uses all of the information available to discriminate one stimulus from another. If the information from the grating is aliased to a lower spatial frequency, the ideal decision rule simply constructs a weighting function to detect the alias. This result is consistent with Williams' (1985a,b) observation that the adult foveal CSF extends smoothly beyond the Nyquist frequency of 60 cpd to nearly 180 cpd once the optics of the eye are bypassed by laser interferometry.[3] The fact that discrimination performance in a contrast sensitivity experiment is not necessarily limited by the Nyquist sampling frequency of the receptor lattice is significant because all too often researchers assume that the Nyquist frequency imposes a hard limit on high-frequency vision (e.g., Jacobs and Blakemore, 1988). Spatially aliased gratings could well attract infants' fixations in forced-choice preferential looking (FPL) experiments and drive visual evoked potentials (VEPs), so there is no reason to believe that the Nyquist frequency of the receptor lattice can predict or limit infants' performance in these tasks. The more likely culprits are the processes that limit intensity discrimination (e.g., photon noise, internal noise, sampling efficiency) and processes that affect signal strength at high spatial frequencies (e.g., optical quality, receptor aperture). This point is bolstered by the observation that adults' and infants' grating acuity varies greatly with luminance (Shlaer, 1937; Brown et al., 1987; Allen et al., 1992; Coletta and Ethirajan, 1991); the Nyquist frequency of the adult foveal cone lattice is always about 60 cpd, but the highest resolvable spatial frequency drops with decreasing luminance to about 10 cpd at low photopic levels.

NEURAL TRANSFER FUNCTION

Obviously, postreceptoral information processing affects contrast sensitivity as well. Here we consider two of the possible neural transfer functions one could assume and describe their influence on contrast sensitivity. The detection of targets of various spatial frequencies is best modeled by assuming that the visual system possesses bandpass detection mechanisms (e.g., Campbell and Robson, 1968; Blakemore and Campbell, 1969). Let us assume for the moment that these mechanisms differ only in the manner in which they combine information from different receptors, that is, that the levels of noise produced within the circuits serving these mechanisms are identical, that the temporal summation properties of the mechanisms are identical, and so on. Now consider two assumptions about the manner in which the sizes of these mechanisms vary with preferred spatial frequency: (1) the mechanisms might have a con-

3. Williams' result and the one shown in Figure 6-5 would not be observed if all three of the following conditions obtained: (1) if the lattice geometry were perfectly regular; (2) if the grating's orientation was 30 degrees from vertical such that its bars lined up with the smallest spaced columns of receptors; (3) if the grating was presented in sine phase so that, at the Nyquist limit, it would present zero-crossings to each column of receptors. These conditions are not generally met because the lattice is not perfectly regular and the eye moves continually, so a grating is seldom in sine phase with respect to the sensing lattice for the duration of a stimulus presentation.

stant size in degrees; or (2) the mechanisms might have a constant bandwidth in log cycles per degree. The spatial receptive fields of these two mechanisms are shown in Figure 6-6A,B. The dashed line in each figure represents a mechanism tuned to a spatial frequency of F cpd; the solid line represents a mechanism tuned to 2F cpd, twice the frequency of the first. The spatial frequency tuning functions of these mechanisms, obtained by Fourier transformation, are displayed in Figures 6-6C,D. The mechanisms of constant size have different bandwidths (the widths of the tuning curves in Figure 6-6C) but the same peak sensitivity (the heights of the tuning curves). Mechanisms of constant bandwidth have different peak sensitivities. The difference in the peak sensitivities is a consequence of the assumption of square-root law (discussed above): The diameters of mechanisms of constant bandwidth are inversely proportional to preferred spatial frequency, so the areas are inversely proportional to the square of the preferred frequency. According to square-root law, therefore, the peak sensitivity of constant bandwidth mechanisms is inversely proportional to the square-root of the square of preferred frequency; that is, it is inversely proportional to preferred frequency.

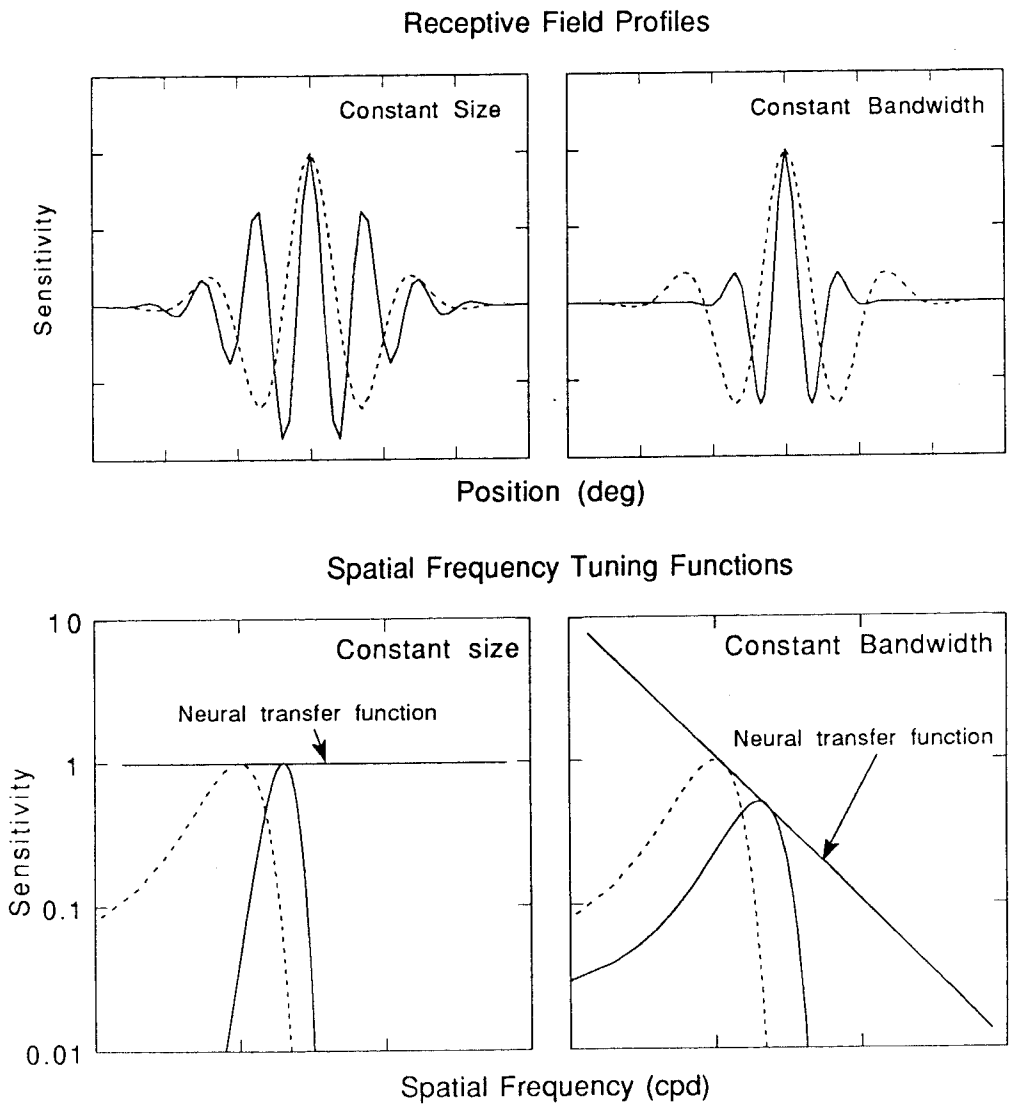

FIG. 6-6. Spatial receptive field profiles and spatial frequency tuning functions for mechanisms of constant size (in degrees) or constant bandwidth (in log spatial frequency). The two upper graphs are the receptive field profiles, and the lower two are the tuning functions. The two graphs on the left are for constant-size mechanisms, and the two on the right are for constant-bandwidth mechanisms. The dashed curves are for a mechanism with a preferred frequency of F, the solid curves for a mechanism with a preferred frequency of 2F. Note that constant-size mechanisms lead to a flat NTF and constant-bandwidth mechanisms to an NTF with a slope of -1.

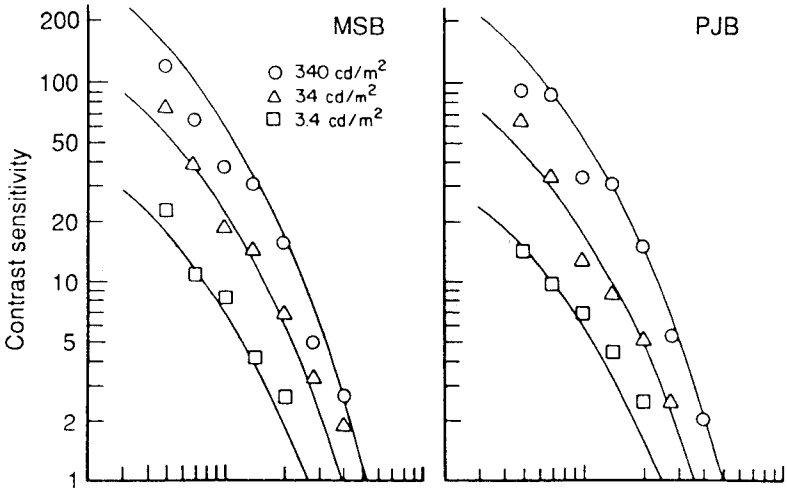

FIG. 6-7. Ideal observer (solid curves) and human (symbols) CSFs for two observers at three luminances from the data of Banks et al. (1987). The data were collected at luminances of 3.4, 34.0, and 340.0 cd/m²; the ideal observer CSFs are for the same luminances. The ideal CSFs have been shifted down by a single scale factor for each observer. The fact that the curves have the same shape indicates that variation in human performance with spatial frequency can be explained by the factors built into the ideal observer; the fact that human and ideal observers show similar variation in sensitivity with luminance indicates that human observers follow square-root law over this range of spatial frequencies and luminances.

The CSF of a system limited by the neural transfer function only is shown in Figure 6-6 for constant size and constant bandwidth mechanisms. Note again that under the constant size assumption the contrast sensitivity of the system is independent of spatial frequency, and under the constant bandwidth assumption the sensitivity of the system is inversely proportional to spatial frequency.

PREDICTING ADULT DATA

Before turning to development, it is important to consider how the factors shown in Figure 6-1 affect contrast sensitivity in mature visual systems. Banks et al. (1987) used an ideal decision rule applied in the fashion suggested by Figure 6-1 to calculate the best possible contrast sensitivity the human adult fovea could have given the constraints of the processing stages shown. The values they used for each of the factors discussed above are given in Table 6-1. In a sense, Banks et al. (1987) assumed a constant bandwidth NTF because they restricted the ideal observer to detection of gratings with a fixed number of cycles. Therefore the ideal observer used weighting functions such as those of Figure 6-6A to make detection judgments.

Banks and colleagues also measured contrast sensitivity psychophysically in two adult observers under the same conditions presented to the ideal observer. Figure 6-7 displays the ideal and human adult CSFs. The data points are contrast sensitivities from 5 to 40 cpd collected at 3.4, 34, and 340 cd/m². As expected, contrast sensitivity declines monotonically from medium to high spatial frequencies, and sensitivity is greater for high than for low luminances. The solid lines are the ideal CSFs for the same stimulus conditions, shifted downward as a unit (by 1.33 log units for observer M.S.B. and 1.43 log units for P.J.B.) to fit the data. The similarity of shapes demonstrates that the high-frequency rolloff of the adult foveal CSF can be explained by consideration of information losses among the factors discussed above, assuming a constant-bandwidth NTF.[4] This observation implies in turn that efficiency beyond the last stage shown in Figure 6-1 is constant from 5 to 40 cpd for adult foveal vision. The fact that real and ideal CSFs are affected similarly by changes in luminance implies that square-root law holds under these conditions and that efficiency beyond the last stage shown in Figure 6-1 is constant across this range of photopic luminances. It is important to note that the similarity in shapes between the human and ideal CSFs breaks down at low spatial frequencies where lateral interactions not incorporated in the ideal observer affect contrast sensitivity (Crowell and Banks, in preparation). We return to the modeling of low-frequency sensitivity later.

4. For gratings of fixed size (in degrees), the high-frequency slope of the ideal CSF is shallower than the observed slope because the ideal weighting function incorporates information from all available grating cycles, but human adults do not appear to summate information across all cycles.

Tracking information losses through the front-end stages shown in Figure 6-1 by using an ideal observer analysis allows one to predict the high-frequency rolloff of the adult CSF. Having shown the independent effects on contrast sensitivity of all the front-end processing stages, we now turn to development and the models of Banks and Bennett (1988) and Wilson (1988) (see also Chapter 32). We develop three models: the Banks and Bennett model in the framework of the above discussion, the Wilson model, and a modified version of the Wilson model incorporating more realistic assumptions.

BANKS AND BENNETT ANALYSIS OF DEVELOPMENT

Developmental Changes in Optics, Pupil, and Media Transmittance

Banks and Bennett (1988) examined the influence of eye growth and receptor maturation on the development of acuity and contrast sensitivity. They first examined the four optical properties that are important to the transmission of signals into the retinal image: eye size (specifically, posterior nodal distance), numerical aperture (pupil diameter divided by focal length), ocular media transmittance, and the OTF. The newborn's eye is significantly smaller than that of the adult. Because image magnification is proportional to the posterior nodal distance of an eye (the distance between the "center point" of the optics and the retina), an object of a given size projects to a smaller area on the retina (expressed in millimeters) in the newborn than in the adult. Banks and Bennett (1988) reported the posterior nodal distances of the newborn and adult eyes as 11.7 and 16.7 mm, respectively, a ratio of 1.43 (the adult/15-month-old ratio is about 1.16). Thus the retinal image of a small object is 1.43 times greater in the adult eye than in the newborn eye (when the image size is expressed in millimeters), a fact that should favor fine detail vision in the adult. In terms of the equations described above, in which all factors are expressed in degrees, it has the effect of enlarging the newborn's receptor aperture $[r(x, y)]$ and spacing $[s(x, y)]$.

Two factors affect the proportion of photons incident on the cornea that make it to the retina: the numerical aperture of the eye (P), and the transmittance of the ocular media (T). Retinal illuminance is proportional to the eye's numerical aperture. The newborn pupil is smaller than that of the adult: According to Salapatek and Banks (1978), 1-month-old and adult diameters at 66 cd/m^2 are 2.4 and 3.9 mm, respectively. However, the numerical apertures of the two eyes are similar because the age-related increase in pupil diameter is offset by the increase in posterior nodal distance (Dannemiller and Banks, 1983; Brown et al., 1987). Consequently, we assumed that the retinal illuminance associated with a given target luminance does not change with age. Two elements affecting ocular media transmittance are known to change with development: the crystalline lens and macular pigments. In both cases transmittance is probably higher in the young eye (Bach and Seefelder, 1914; Werner, 1982; Bone et al., 1988), but the differences are small at all but short wavelengths. Banks and Bennett (1988) built differences in media transmittance into their calculations mostly because they examined some hue discriminations involving short wavelengths; here we assume the media transmittance is constant with age because we are concerned with spatial vision and broadband lights only. Thus we assume that the retinal illuminance associated with a given target luminance is the same in newborns and adults (i.e., P and T are the same).

No measurements of OTF $[O(u, v)]$ of the human newborn have been reported, but it is likely that the optical quality of the newborn eye greatly exceeds the resolution performance of the visual system as a whole. Banks and Bennett (1988) assumed therefore that the OTF is adult-like at birth, and we follow that assumption here by using adult OTFs from Campbell and Gubisch (1966) for all ages.

Retinal Development

Banks and Bennett (1988) also considered the effects of receptor maturation. Several investigators have reported that the retina is immature at birth, particularly in and around the fovea (Bach and Seefelder, 1914; Abramov et al., 1982; Hendrickson and Yuodelis, 1984; Yuodelis and Hendrickson, 1986). For instance, the diameter of the rod-free area of the retina decreases from about 5.4 degrees at birth to 2.3 degrees at maturity, a developmental change that is apparently the consequence of postnatal migration of foveal cones toward the center of the retina. Figure 6-8 shows tangential sections of the retina near the center of the fovea at birth, 15 months, and adulthood. An individual cone is outlined for clarity in each photograph. As one can see, the foveal cones of the newborn human are strikingly immature: Neonatal inner segments are much broader and shorter than their mature counterparts, and neonatal outer segments are much shorter than the adult versions. The cones of the retinal periphery are also immature at birth (see Chapter 17), but the differences between young and old versions are not as distinct as in the fovea.

In the adult, the inner segment of a foveal cone acts as a funnel, gathering light and guiding it to the outer segment where it isomerizes the photopigment. Banks and Bennett (1988) calculated the ability of the new-

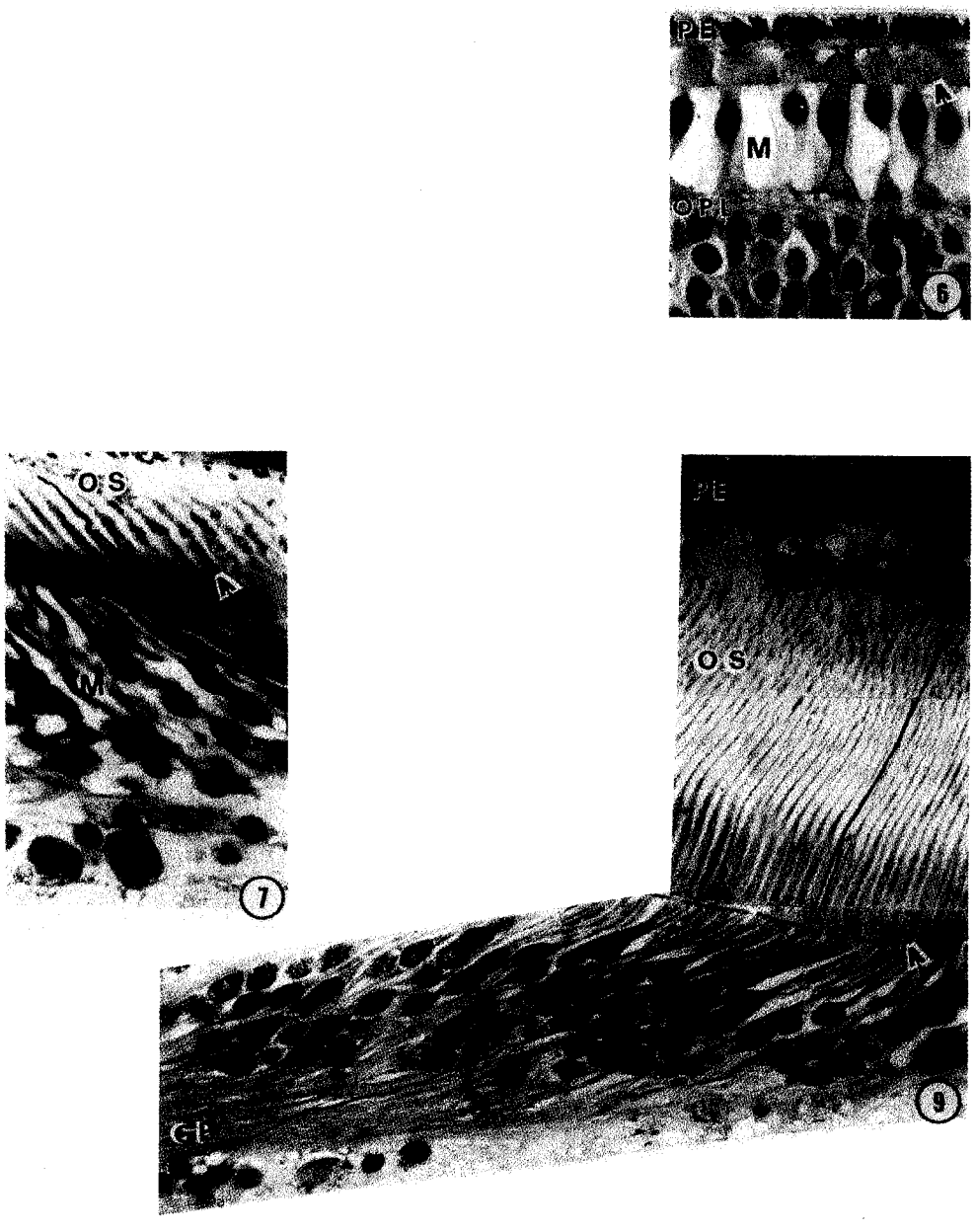

FIG. 6-8. Tangential sections of the retina near the center of the fovea at birth, 15 months, and adulthood. The magnification is the same in each panel. An individual cone is outlined for clarity in each photograph. The outer segments of the receptors are labeled OS, and the inner segments are just below the outer segments. See text for further discussion.

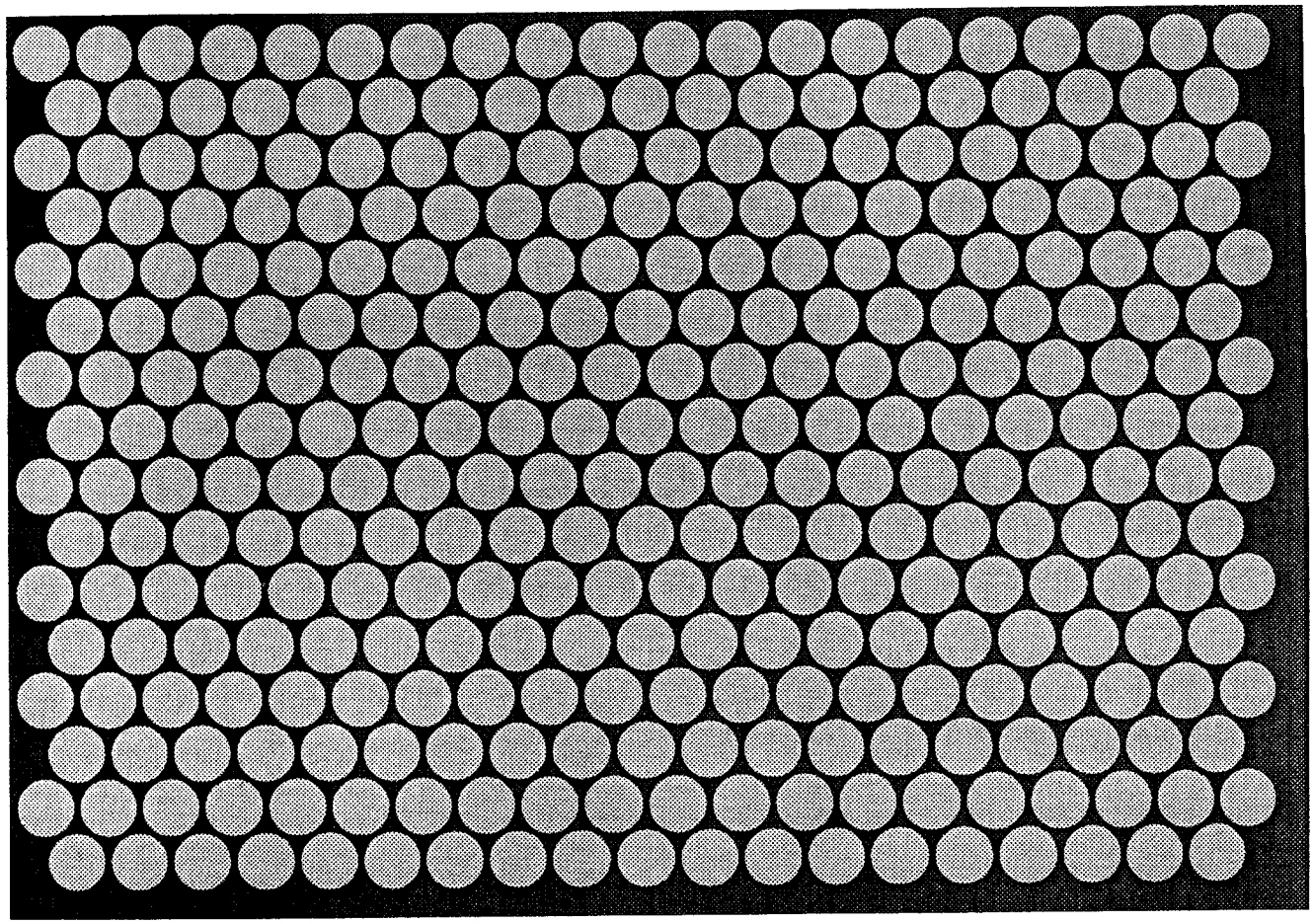

FIG. 6-9. Foveal cone lattices for (a) an adult and (b) a newborn. The white bars represent 0.5 minute. The gray areas represent the effective light collecting areas, that is, the receptor apertures. See text for further discussion.

born's foveal cone inner segments to perform this function. They concluded that the funneling or waveguide property of the immature inner segment cannot work properly; any photons that are not aimed directly at an outer segment are not absorbed. In other words, the effective aperture of newborn foveal cones appears to be the outer segment itself, a conclusion also reached by Brown et al. (1987) and Wilson (1988; see Chapter 32). Taking the smaller size of the newborn's eye into account, the angular diameter of the effective aperture—the outer segment—is approximately 0.35 minute. The effective aperture of adult foveal cones is, of course, the inner segment and is about 0.48 minute (Miller and Bernard, 1983; MacLeod et al., 1992). The effective aperture at 15 months is probably the inner segment, and its diameter is about 0.67 minute.

Banks and Bennett (1988) also calculated the average spacing between foveal cones, assuming a regular hexagonal arrangement. Based on the anatomical data of Yuodelis and Hendrickson (1986), they reported values of 2.3, 1.27, and 0.58 minutes in the newborn, 15-month, and adult central foveae, respectively. The spacing changes are a consequence of receptor migration and increasing eye size. The Nyquist frequencies associated with such lattices are given by $1/\sqrt{3} * d$) (Snyder and Miller, 1977) and are 15.1, 27.2, and 59.7 cpd for newborns, 15-month-olds, and adults, respectively.

These intercone distances and effective aperture diameters were used to construct the receptor lattices shown in Figure 6-9. The white bars represent 0.5 minute. The gray areas represent the effective light-collecting areas, that is, the receptor apertures. The effective collecting areas cover 2% of the fovea in newborns, 25% in 15-months-olds, and 62% in adults. Clearly, most incident photons are not collected within newborn cone apertures.

The efficiency of the outer segment (E)—that is, the proportion of photons striking the outer segment that are absorbed—also varies between neonates and adults. As shown in Figure 6-8, the lengths of newborn and

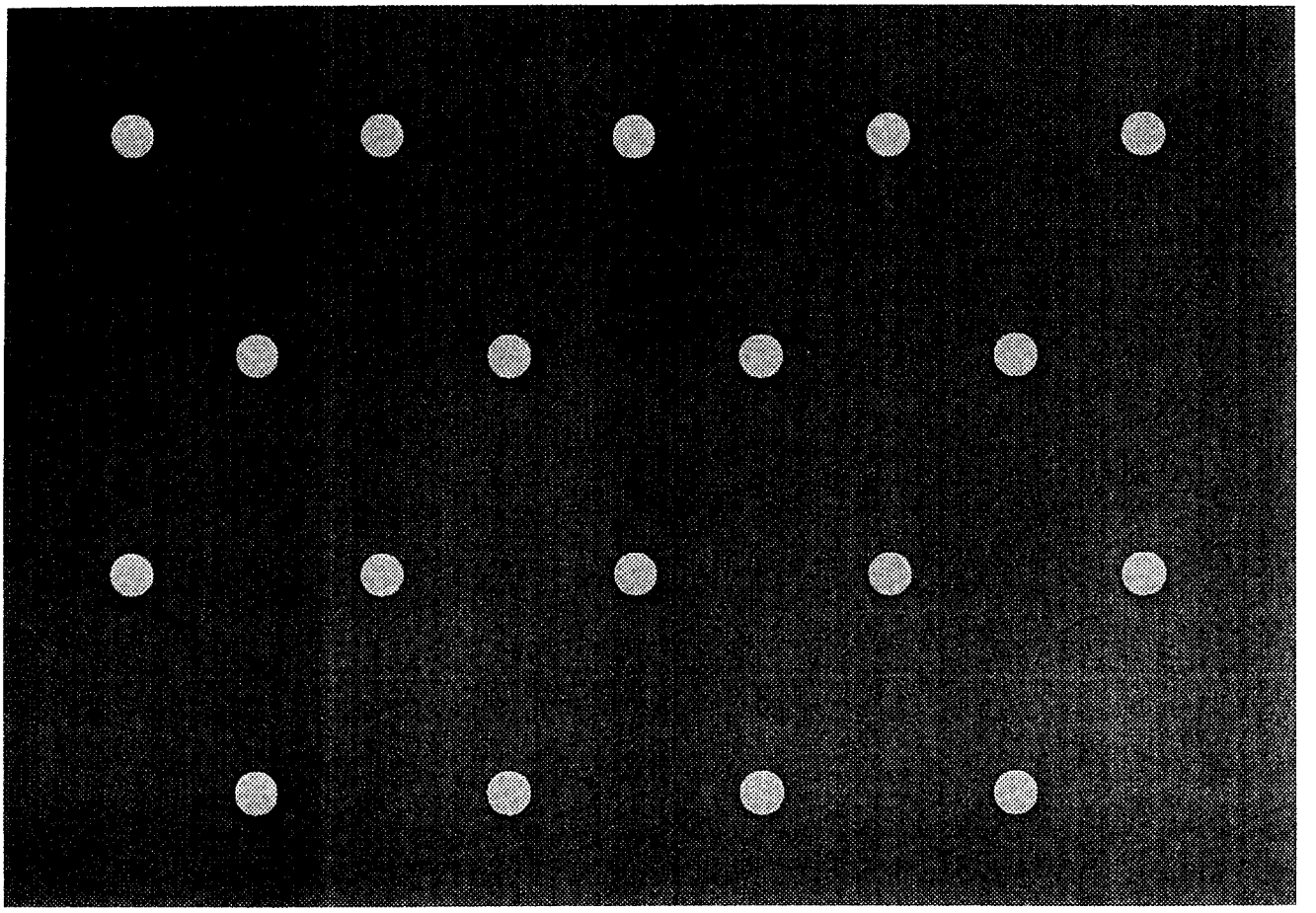

B 7.3 mm

FIG. 6-9. (*continued*)

adult outer segments differ substantially. In the cental fovea, the adult/newborn lengths ratio is about 16:1 and adult/15-month lengths ratio is about 2.2:1. Banks and Bennett assumed that the newborn and adult outer segments differ only in their widths and lengths (i.e., the photopigment concentrations and extinction coefficients are the same). They used Beer's law[5] to estimate the proportions of incident photons that produce isomerizations (Wyszecki and Stiles, 1982). By their calculations, the 16:1 and 2.2:1 path length ratios produce 10:1 and 1.8:1 ratios of the number of isomerizations for a given number of incident photons.

Taking into account the age-related changes in the factors discussed above and listed in Table 6-1, Banks and Bennett (1988) estimated that the adult central foveal cone lattice absorbs 350 times more photons than does the newborn lattice and four times more photons than the 15-month-old lattice. Stated another way, if identical patches of light are presented to newborn and adult eyes, roughly 350 photons are effectively absorbed in adult foveal cones for every photon absorbed in newborn cones. Because an ideal decision rule is used, the modeling of Banks and Bennett follows square-root law. Thus the 350-fold loss in newborns' photon catch should produce a roughly $\sqrt{350}$ (18.7-fold) drop in contrast sensitivity, and the fourfold loss in the 15-month catch should produce a twofold drop.

To summarize, Banks and Bennett (1988) assumed that four front-end properties of the visual system change with increasing age. (1) Image magnification increases with eye growth. (2) The effective receptor aperture $[r(x, y)]$ increases in size as the inner segment begins to act as a funnel. (3) The receptor spacing $[s(x, y)]$ decreases as cones migrate toward the fovea. (4) The efficiency of the outer segment (E) increases as it grows longer. As stated above, the consequence of increased image magnification is to decrease the aperture size and spacing of the receptors expressed in angular units.

5. The number of absorptions is equal to $k * (1 - 10^{c \cdot e \cdot l})$, where c = pigment concentration, e = extinction coefficient, l = segment length, and k = a constant.

Therefore the effects of these four developmental factors on Eqs. 1 and 2 are to: (1) make the newborn receptor aperture slightly smaller, decreasing its diameter from the adult value of 0.48 minute (Miller and Bernard, 1983) to about 0.35 minute; (2) increase the spacing between newborn cones from 0.58 minute to 2.3 minutes; and (3) decrease the newborn outer segment efficiency by a factor of 10. The 15-month aperture at 0.67 minute is actually larger than that in the adult; the 15-month values for the other factors fall between the neonatal and adult values but are closer to those of the adult.

In the next sections, we isolate these three effects and show, step by step, how they affect contrast sensitivity. As above, we do it by placing an ideal decision rule at the output of the schematic visual system in Figure 6-1 and varying the parameter under consideration while holding other parameters fixed.

Consequences of Age Changes in Outer Segment Efficiency

The effect of age-related changes in the outer segment efficiency (E) is shown in Figure 6-10. As in Figure 6-2, we assumed experimental conditions similar to those under which infant CSFs have been measured. Space-average luminance was 50 cd/m^2, large grating patches were used, and the pupil was natural with a diameter of 6 mm. The target duration was 250 ms, and threshold was the contrast required to achieve 71% correct, in a two-interval, forced-choice procedure. For construction of Figure 6-10, the OTF [$O(u, v)$] and NTF [$N(u, v)$] were flat, and receptor spacing [$s(x, y)$] and aperture diameter [$r(x, y)$] were set to 0.58 and 0.48 minute, respectively, the values in the adult fovea. Media transmittance (T) and numerical aperture (P) were set to adult values for the fovea (Table 6-1). The curves show the contrast sensitivity of a system with an ideal decision rule when the adult, 15-month, and neonate outer segment efficiencies are those reported by Banks and Bennett (1988) and reproduced in Table 6-1.

Consequences of Age Changes in Receptor Spacing and Aperture

Figure 6-11 illustrates the effect of changes in receptor spacing and the diameter of the receptor aperture. Here peak sensitivity is normalized to 1 for the adult system, and the neonate and 15-month sensitivities are plotted relative to those values. When constructing this figure, the media transmittance and numerical aperture were set to adult values, the OTF and NTF were flat, and the outer segment efficiency was set to adult values. The figure shows that coarse receptor spacing and small receptor apertures in the neonate lead to reduced sensitivity for an otherwise ideal system. The 15-month sensitivity falls between that of the adult and the neonate.

Combined Effects

Figure 6-12 shows the CSFs once all the factors are included. At all ages, we assumed adult values for media transmittance, numerical aperture, and optical transfer [3.8 mm data of Campbell and Gubisch (1966)]. We also assumed a constant-bandwidth NTF. We then plugged in the age-appropriate values for receptor spacing, receptor aperture, and outer segment efficiency once the effect of image magnification had been incorpo-

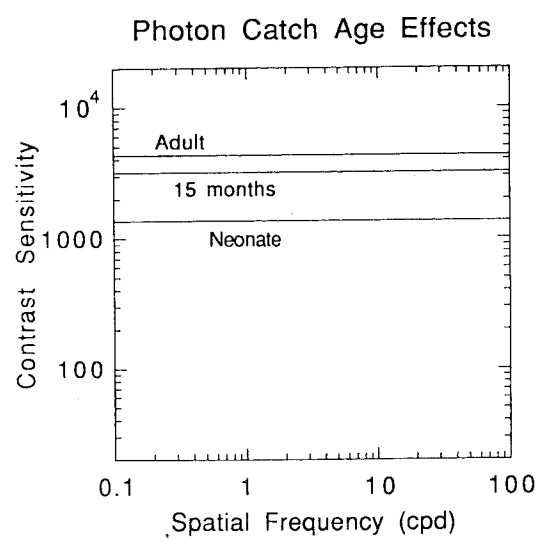

FIG. 6-10. Effect of age-related changes in the outer segment efficiency (E) on contrast sensitivity. See text for explanation.

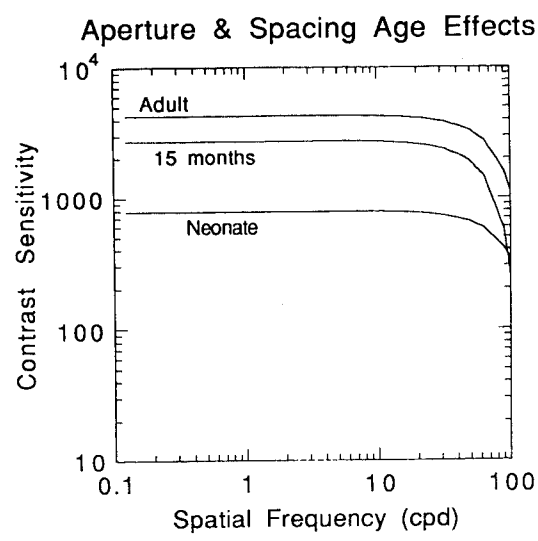

FIG. 6-11. Effect of age-related changes in receptor spacing and the diameter of the receptor aperture. See text for explanation.

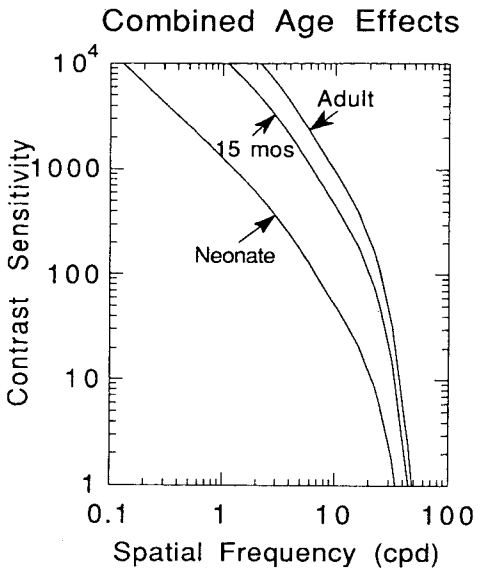

FIG. 6-12. CSFs once all factors are included. See text for explanation.

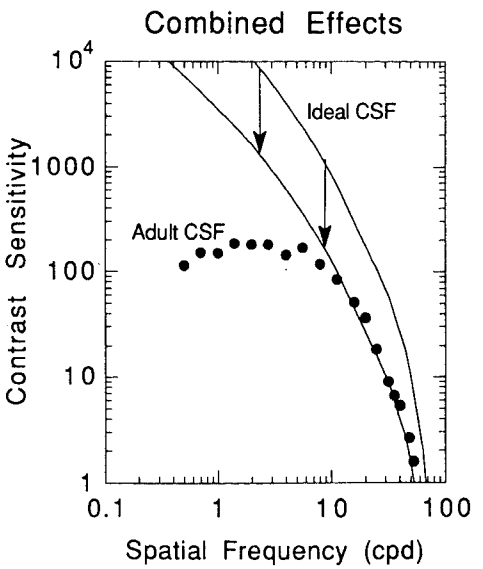

FIG. 6-13. Human adult and ideal CSFs. The data points represent the contrast sensitivity of observer M.S.B., which was measured at 50 cd/m^2, with large grating patches, 250 ms target duration, natural pupil of 6 mm, and 21FC procedure. The ideal CSF is for the same conditions, assuming mechanisms of constant bandwidth. The ideal CSF, once shifted downward by 1.4 log units (indicated by arrows), fits the data reasonably well from 6 to 60 cpd.

rated. The resulting CSFs are those of ideal observers, limited by the factors incorporated, for the assumed experimental conditions. There are clear developmental differences in the resulting CSFs; the neonatal CSF is essentially the same as the adult CSF shifted down by a factor of 18.7 ($\sqrt{350}$). The 15-month CSF falls between those of the neonate and the adult; it is nearly equivalent to an adult CSF shifted down by a factor of 2.

The differences among these functions represent the presumed consequences of information losses due to lower image magnification and the reduced photon catch that stems from greater receptor spacing, smaller receptor apertures, and lower outer segment efficiency. The differences are large, but are they large enough to account for the observed differences between real neonates and adults? To answer this question, let us evaluate a specific hypothesis.

> *Developmental hypothesis:* Spatial contrast information losses are the same in neonatal and adult visual systems except for the losses caused by reduced image size and reduced photon catch resulting from receptor immaturities.

To evaluate this hypothesis, we conducted an experiment in which we measured the CSF of an experienced adult observer under conditions such as those used to measure CSFs in infants. The conditions were the same as those assumed for the construction of the ideal CSFs of Figures 6-2 through 6-5: two-interval, forced-choice procedure, large grating patches, luminance of 50 cd/m^2, duration of 250 ms, and natural pupil diameter of 6 mm. The resulting CSF is shown in Figure 6-13.

Figure 6-13 also shows the ideal CSF for the same conditions. Note that the ideal CSF is about 0.7 log units higher than the empirical one across a broad range of spatial frequencies. However, when the ideal CSF is shifted downward, as shown by the arrows, it fits the empirical function well from 5 to 60 cpd, a result consistent with the earlier observations of Banks et al. (1987). Thus we can fit the observed contrast sensitivity data across a broad range of spatial frequencies if we assume that the processes not included in our analysis simply cause a uniform 0.7 log unit loss of contrast sensitivity.

If the developmental hypothesis stated above is correct—that information losses in the neonatal and adult visual systems are the same except for losses due to the immaturities incorporated in the model—we should be able to fit the neonate's empirical CSF by shifting the age-appropriate ideal CSF downward by the same 1.4 log units required to fit the adult data. We have done so in Figure 6-14. We have also plotted the behavioral data of Banks and Salapatek (1978) and the electrophysiological data of Norcia et al. (1990). The functions of Norcia et al. were collected at 220 cd/m^2, so we have shifted them downward according to square-root law to make them comparable. It is clear that the shifted ideal CSFs do not fit the observed data; much larger shifts than predicted by the Banks and Bennett (1988) analysis would be required to fit the data. We conclude, as did Banks and Bennett, that information losses among the front-end mechanisms they modeled are insufficient to account for the observed sensitivity deficits. The de-

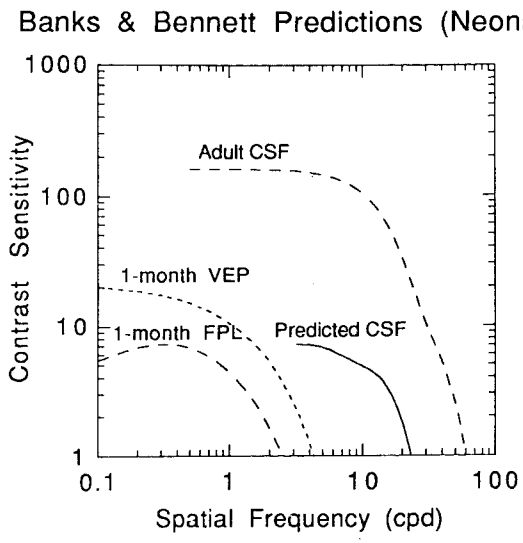

FIG. 6-14. Banks and Bennett neonate prediction and observed infant CSFs. The upper curve is the adult CSF used as a starting point for the modeling. The curve is the neonate prediction under the assumption that square-root law holds. As in Banks and Bennett (1988), the predictions have not been extended to low spatial frequencies, where square-root law does not hold in adults. The dotted curve represents 1-month VEP data from Norcia et al. (1990) and the dashed curve 1-month FPL data from Banks and Salapatek (1978). The preretinal, age-related changes considered by Banks and Bennett clearly do not account for the low contrast sensitivity observed in neonates.

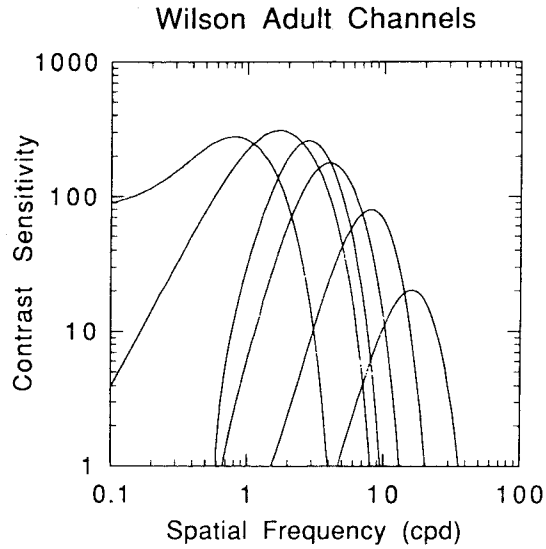

FIG. 6-15. The six spatial-frequency-tuned channels of Wilson's model of adult spatial vision. The bandwidths of the channels were determined using a masking technique (Wilson et al., 1983); their vertical positions have been shifted to fit the adult VEP CSF of Norcia et al. (1990). Wilson's model of human visual development (Wilson 1988, see Chapter 32) consists of a set of transformations that are applied to these six functions.

velopmental hypothesis we entertained earlier is therefore false. Immaturities must exist at other stages of visual processing that are significant enough to limit performance more in neonates than those stages do in adults. Thus the earlier hypothesis must be replaced by one that states that postreceptoral immaturities also contribute significantly to the contrast sensitivity deficits observed early in life.

WILSON MODEL OF DEVELOPMENT

Description of the Model

Wilson's (1988; see Chapter 32) analysis has both similarities and dissimilarities to the Banks and Bennett (1988) analysis. His analysis is based on a model of adult contrast sensitivity and on two simple assumptions about human ocular and retinal development. The model of adult sensitivity incorporates the six spatial-frequency-tuned channels shown in Figure 6-15. The adult CSF is the envelope of the sensitivities of these six channels. The sensitivities have been shifted vertically to fit the adult VEP contrast sensitivity data of Norcia et al. (1990).

In his developmental model, Wilson transformed the channels of the adult model according to his assumptions about the developmental factors that have important effects on spatial visual tasks. Wilson assumed that only two significant developmental changes occur: (1) the photoreceptor outer segments become longer and hence absorb more of the incident photons; and (2) the photoreceptors move closer together allowing the adult visual system to signal higher spatial frequencies more accurately.

To incorporate the first factor, Wilson simply assumed that both the adult and infant visual systems follow square-root law at all spatial frequencies. He calculated that the adult's outer segment captures 7.2 times more photons than does that of the neonate; thus the effect of outer segment growth is to increase adult sensitivity by a factor of $\sqrt{7.2}$, or 2.7 relative to the neonate, independent of spatial frequency.

The implementation of the second factor is more complicated. Wilson made the following assumptions: (1) neonate foveal cones are 4.6 times farther apart than adult foveal cones; (2) the connections between cones and higher-order neurons do not change over the course of development, so a given higher-order neuron takes inputs from the same number of photoreceptors with the same weightings in neonates and adults; and (3) the size of the photoreceptor aperture (in degrees) does not change with age. These three assumptions have the following consequence: For a grating imaged on the retina, the neonate should have a 2.7 times lower sensitivity to a given spatial frequency as has the adult for a grating of a frequency 4.6 times higher. Figure 6-16A represents

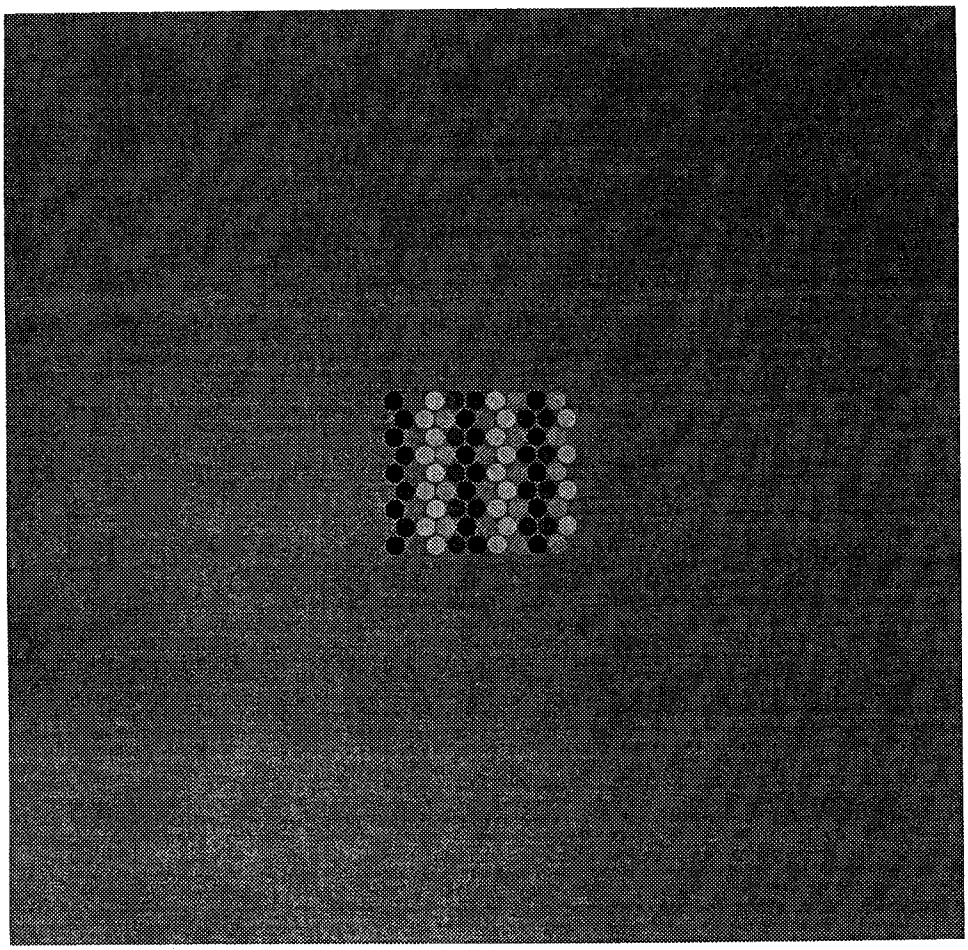

A

FIG. 6-16. Principle behind Wilson's horizontal shift. Circles represent individual receptor apertures, the gray value of each circle corresponding to the photon catch when a grating is presented. (A) Pattern of photon catches for an adult lattice (spacing equals 0.58 minute) when stimulated by a 30 cpd grating. (B) Photon catches when a neonatal lattice (spacing equals 0.58 × 4.6, or 2.67 minutes) is stimulated by a 6.5 cpd grating.

a photoreceptor lattice, with the receptors lined up with the peaks and troughs of a sinewave. The circles represent individual cones, with the intensities representing their photon catches. Figure 6-16B represents a lattice in which the receptors are 4.6 times farther apart; the photoreceptors line up with the peaks and troughs of a grating with a frequency 4.6 times higher than the grating in Figure 6-16A. When constructing the figure, we assumed that the eye's optics passed the two gratings equally well. Clearly, the spatial patterns of photoreceptor responses are identical in the two cases. If the photoreceptors catch the same number of photons (i.e., if they have the same aperture size), the total number of photons available to detect the sine wave is the same, and sensitivity should be equal in the two cases. This shift of sensitivity to lower spatial frequencies in the neonate is represented in Wilson's original model (Wilson, 1988) by a rigid 4.6-fold shift on the log-frequency axis of the adult channels to the left.

There is a complicating factor, however: Not all spatial frequencies are transmitted to the retina with equal fidelity. As described earlier in the chapter, the optics of the eye and the receptor aperture act as low-pass filters, severely attenuating the contrasts of high-frequency targets. These effects must be taken into account before the horizontal shift is applied. Wilson's original model did not take them into account, so the predicted acuities and contrast sensitivities were erroneous. In his revised model (see Chapter 32), the effects were taken into account as we describe here. To represent the attenuating effect of the optics, Wilson assumed a simplified version of an OTF [$O(u, v)$] described by Geisler (1984) for a pupil diameter of 2 mm. He discussed the receptor aperture and its low-pass filtering

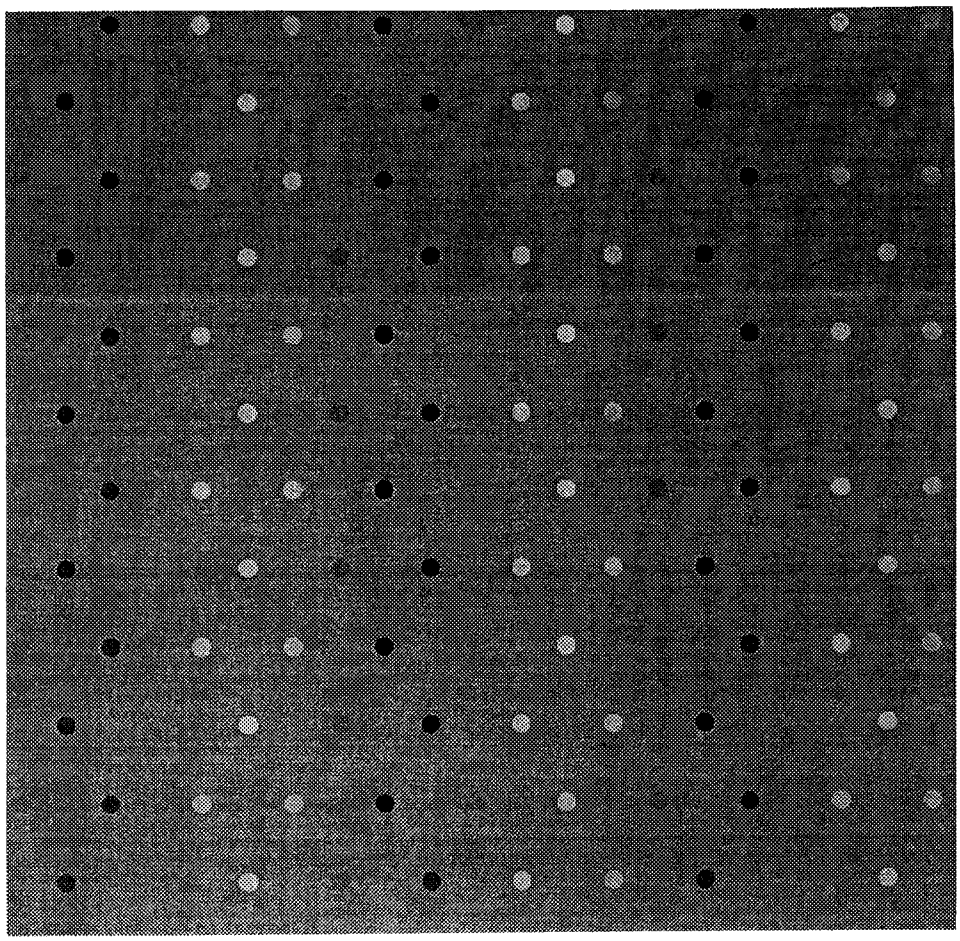

B

FIG. 6-16. (*continued*)

effects but chose to ignore it because the effects are small at the spatial frequencies of interest here. To determine the sensitivity of his adult model to retinal image contrast, Wilson divided the channel sensitivities by the OTF. This operation is illustrated in Figure 6-17. The dashed curves are the channel sensitivities from Figure 6-15, and the solid lines are the sensitivities after division by the OTF. They represent the channel sensitivities to retinal image contrasts rather than to external stimulus contrasts. The effect is to raise sensitivity to high frequencies.

To represent the consequence of cone migration, Wilson then applied a rigid shift to the left. The effect is illustrated in Figure 6-18; again the dashed curves represent the positions of the channels from the previous figure. He next put the optics back in. Wilson assumed that infant and adult OTFs are identical, so it involved multiplying the channels obtained from the prior steps by the same OTF. The 2-mm OTF is nearly flat with a value of about 1 from 1–10 cpd; hence this operation has little effect. In other words, by this set of assumptions, the shape of the neonate's CSF is determined almost entirely by the shape of the NTF.

Finally, to account for the neonate's shorter outer segments, Wilson divided the channel sensitivities by 2.7, as shown in Figure 6-19. The envelope of the resulting curves represents Wilson's prediction for the neonate's CSF. A similar sequence of operations with different parameters led to his predicted CSF for 15-month-olds.

Figure 6-20 shows Wilson's predicted CSF along with the infant CSF data of Norcia et al. (1990) and Banks and Salapatek (1978). The prediction matched the Norcia data at 2 months rather well but did not match Norcia's 1-month data or Banks and Salapatek's 1- or 2-month data; the younger infants' sensitivity was simply lower than predicted. Thus Wilson's model with parameters from neonatal anatomy does not fit neonatal data.

Figure 6-21 shows Wilson's predicted CSF for 15-month-olds along with the 8-month data from Norcia et al. (1990). The predicted and observed functions are

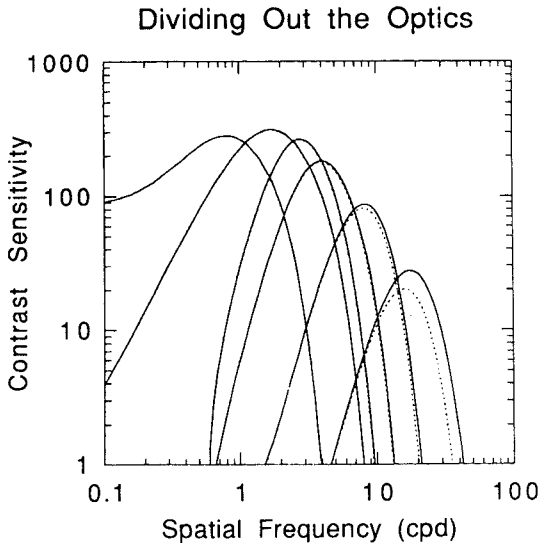

FIG. 6-17. First transformation of Wilson's (see Chapter 32) model: dividing out the OTF. Dotted and solid curves represent the positions of the channels before and after the transformation; the dotted curves are largely obscured because the transformation has no effect at low spatial frequencies. The envelope of the solid curves corresponds to the adult NTF; note that the cutoff point of the NTF implies that there is a neural limit that makes adults incapable of detecting frequencies higher than 42 cpd (at luminances around 220 cd/m^2), contradicting the results of Williams (1985b) (see text).

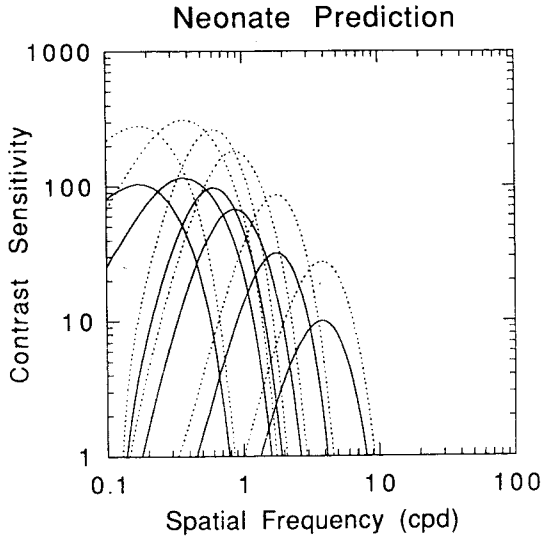

FIG. 6-19. Third and fourth transformations of Wilson's model (see Chapter 32): multiplying by the neonate OTF and incorporating the effect of reduced outer segment length. The neonate OTF is assumed to be identical to that of the adult, which Wilson assumed is flat with a value of about 1.0 to around 10.0 cpd; multiplying by this OTF therefore has little effect. The effect of reduced outer segment length is a rigid downward shift by a factor of 2.7. Again, the dotted and solid curves represent the positions of the channels before and after the transformation. The envelope of the solid curves here corresponds to the predicted neonate CSF.

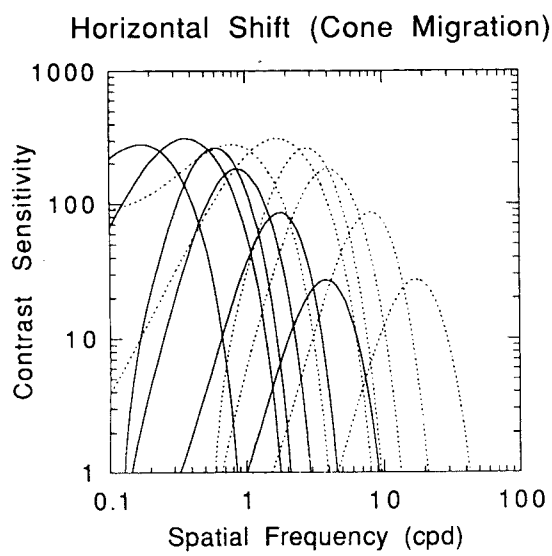

FIG. 6-18. Second transformation of Wilson's model (see Chapter 32): a rigid leftward shift by a factor of 4.6, reflecting the effect of photoreceptor migration. As in Figure 6-17, the dotted and solid curves represent the positions of the channels before and after the transformation. The envelope of the solid curves here corresponds to the neonate NTF.

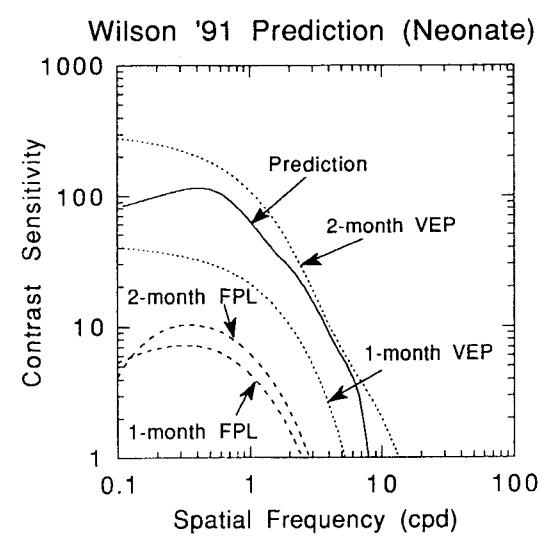

FIG. 6-20. Wilson's prediction for neonates (solid curve) and some observed CSFs (see Chapter 32). The dotted curves are functions fit to data of Norcia et al. (1990); the data were collected at 1 and 2 months using a sweep-VEP technique. The dashed curves are functions fit to FPL data collected by Banks and Salapatek (1978) at 1 and 2 months. Although the VEP and FPL data were collected at different luminances, they have not been shifted in this figure (unlike in Figure 6-14). The Wilson prediction is close to the 2-month VEP CSF, but this comparison is not appropriate because the model prediction should be compared only to the 1-month data. Even before modifying Wilson's assumptions, the model does not fit the data.

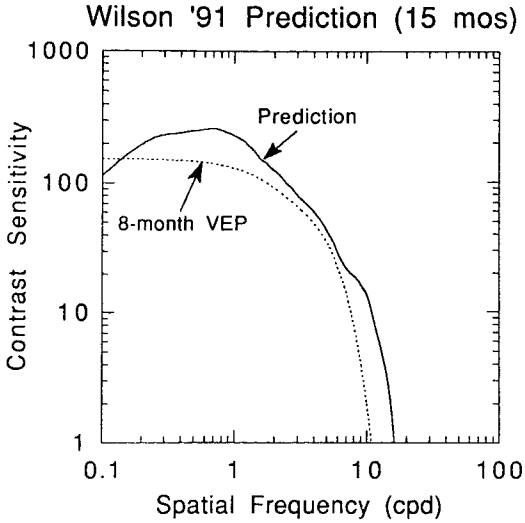

FIG. 6-21. Wilson's (see Chapter 32) 15-month prediction (solid curve) and an observed CSF. The dotted curve is a function fit to the data of Norcia et al. (1990); the data were collected at 8 months using a sweep-VEP technique. The fit is good before we modify Wilson's assumptions.

reasonably similar, but again the match occurs at different ages for the model and data. Wilson (see Chapter 32) also derived grating acuity predictions from his predicted contrast sensitivities and claimed that they matched the observations of Norcia et al. (Norcia and Tyler, 1985; Norcia et al., 1989) reasonably well near the end of the first year and moderately well during the first month. He concluded, therefore, that the major contribution to poor contrast sensitivity early in life is immaturities among front-end mechanisms.

Evaluation of the Wilson Model

When developing his model, Wilson made some assumptions that strike us as questionable: (1) the choice of data to which the adult model was fit (Norcia et al. 1990) to establish the starting point for the modeling; (2) that square-root law holds at all spatial frequencies at the illuminances at which the studies were run; (3) that the eye's optics in those studies are well represented by the OTF for a 2 mm pupil (Fig. 6-3); and (4) that the size of the photoreceptor aperture (in degrees) does not change with age. In this section, we discuss the problems with these assumptions. Later, we develop a version of Wilson's model incorporating assumptions that we think are more plausible.

Choice of Data Sets. The choice of data sets to represent adult and infant contrast sensitivities is important. The experimental conditions under which adults and infants were tested should be as similar as possible and should be consistent with as many modeling parameters as possible.

When making the decision, one must consider the response measure. One could use behavioral techniques, such as the forced-choice preferential looking method (FPL) (Teller, 1979), or electrophysiological techniques, such as the sweep VEP (Norcia and Tyler, 1985). In the case of behavioral techniques, one must worry about differing effects of attention span in the adult and infant and other task variables that might affect performance (such as whether the method of adjustment or a two-alternative, forced-choice procedure was used in the adult). In the case of electrophysiological techniques, one must consider several effects that might change with age, such as signal conductance through the skull and sensitivity to different temporal frequencies.

Wilson (1988; see Chapter 32) used VEP estimates of adult and infant CSFs, according to Norcia et al. (1990), as the data to be modeled. Their choice may be the best one because the method used to determine sensitivity is identical in infants and adults; it does bring with it a problem, however. In infants sweep VEP estimates of sensitivity are generally higher than behaviorally estimated sensitivities, but in adults sweep VEP estimates are generally *lower* than behavioral estimates (Norcia and Tyler, 1985; Norcia et al., 1990; Allen et al., 1992). Some of this age-related difference between the two techniques is almost certainly due to reduced motivation on the infant's part, which presumably affects behavioral measurements more than VEP measurements. Of course, motivational variations are difficult to model quantitatively, which argues for using VEP data. On the other hand, signal conductance through the skull is an important determinant of VEP signal strength; and because adults have thicker skulls than infants, the VEP signal may be more attenuated in mature observers. In our opinion, this conductance effect may well lower adult sensitivity relative to the infant, an effect that should be explicitly included in any model of the development of VEP sensitivity. The omission of this factor makes Wilson's model fit the data better than it should given the factors he considered.

Also when choosing the data set to model, one must consider the stimulus conditions: the luminance, size, duration, and flicker rate of the stimulus, the observer's pupil diameter, the threshold criterion, and more. We discuss this issue in the next two sections.

Assumption of Square-Root Law. The most important of the four questionable assumptions is the one concerning the relation between sensitivity and the number of caught photons. Both Wilson (1988, 1993) and Banks and Bennett (1988) assumed square-root law when calculating the effects of reduced numbers of captured photons on contrast sensitivity. Banks and Bennett restricted their

prediction to spatial frequencies above 3 cpd, but Wilson made predictions for frequencies as low as 0.15 cpd. The problem is that square-root law does not hold at all spatial frequencies and luminances. As van Nes and Bouman (1967), Kelly (1977), and Koenderink and van Doorn (1978) have shown, for every spatial frequency there is a retinal illuminance above which sensitivity ceases to rise with increasing illumination. In other words, the visual system follows Weber's rather than square-root law at sufficiently high illuminances, and the illuminance at which this transition occurs is lower for lower spatial frequencies. Assuming (as Banks and Bennett did) that infants and adults are affected similarly by reductions in the number of available photons, it means that the effect of reduced photon catch due to shorter outer segments and more widely spaced photoreceptors is probably smaller than predicted by Wilson, particularly at low spatial frequencies. We discuss this point in greater depth later for both the Wilson and the Banks and Bennett analyses.

Optics. The third problem concerns the OTF $[O(u, v)]$ Wilson used to represent the effects of the human optics in the Norcia et al. (1990) experiment. This OTF is a simplified version of an equation fit by Geisler (1984) to modulation transfer measurements made by Campbell and Gubisch (1966) for a 2-mm artificial pupil. Geisler's full 2-mm OTF is shown in Figure 6-3; the equation Geisler used is the difference of two gaussians. Wilson argued that because he was primarily interested in predicting acuity, he only needed to use one of the two gaussians: the one extending to higher spatial frequencies. This assumption allowed him to derive a simple analytical expression for his infant acuity prediction, but the assumption is questionable because his infant acuity prediction is down in the region affected by the second, lower-frequency gaussian and because he later went on to predict the entire neonate CSF, the shape of which is certainly affected by the second gaussian. These errors are not significant, however, because they are quantitatively small.

A more serious problem is Wilson's implicit assumption that the pupil diameters of the observers in the experiments of Norcia et al. (1990) were 2 mm. Those experiments were run at a luminance of 220 cd/m^2 with natural pupils. At that luminance, adult pupil diameters are 2.4–4.3 mm, with a mean of about 3.5 mm (Spring and Stiles, 1948). Campbell and Gubisch's (1966) OTF for a 3.8-mm pupil is shown as the solid curve in Figure 6-3. The attenuation of high frequencies is obviously more severe at 3.8 than at 2.0 mm. Consequently, the use of a 3.8-mm OTF, which is more realistic for the experimental conditions under consideration here, has a significant effect on the infant predictions, particularly on the predictions of acuity and high-frequency contrast sensitivity. We show this later.

Receptor Aperture. Wilson assumed that the angular diameter of the receptor aperture is about 0.5 minute and does not change with development, which follows from his assumption that the outer segment is the effective aperture of foveal cones (see discussion of Figure 32-1). The problem is that the effective receptor aperture in the adult fovea is the inner segment, not the outer segment (Miller and Bernard, 1983; MacLeod et al., 1992), and the diameter of the mature inner segment is larger than that of the outer segment. Banks and Bennett assumed that the effective cone apertures are the inner segment in adults and outer segments in neonates; the corresponding diameters are 0.48 and 0.35 minute in adults and neonates, respectively. At 15 months, the receptor aperture is probably the inner segment which, at 0.67 minute, is considerably larger.

The size of the receptor aperture affects the proportion of incident photons that are captured by the receptors and, owing to the low-pass filtering of the aperture $[R(u, v)]$, it affects the high-frequency slope of the CSF. The effects are small, but we include them in the reanalysis of Wilson's model anyway.

DIFFERENCES BETWEEN THE APPROACHES

We now turn to the differences between the Wilson and the Banks and Bennett analyses. Wilson (see Chapter 32) argued that the key difference is the way in which the effects of cone migration are incorporated. Wilson assumed that all connections between photoreceptors and higher neurons are maintained in development, so a neuron responding to a range of low frequencies at birth responds to a higher range at maturity because the receptors that feed it have moved closer together. Thus the effect of tighter receptor spacing with increasing age is a horizontal shift on the log spatial frequency axis. As pointed out by Wilson (see Chapter 32), Banks and Bennett incorporated the spacing effect as a vertical shift. Wilson claimed that it requires that the connections change with age. This statement is false. In fact, given square-root law and the NTFs $[N(u, v)]$ assumed by Banks and Bennett for the adult and the infant, these two methods of implementing the effects of cone migration are exactly equivalent.

To understand, consider a developing visual system in which the only change from birth to maturity is a fourfold decrease in receptor spacing. This shrinking of the photoreceptor lattice would be represented in Wilson's model by shifting the NTF to the right by a factor of 4; in the Banks and Bennett analysis, this lattice would capture a higher proportion of the incident pho-

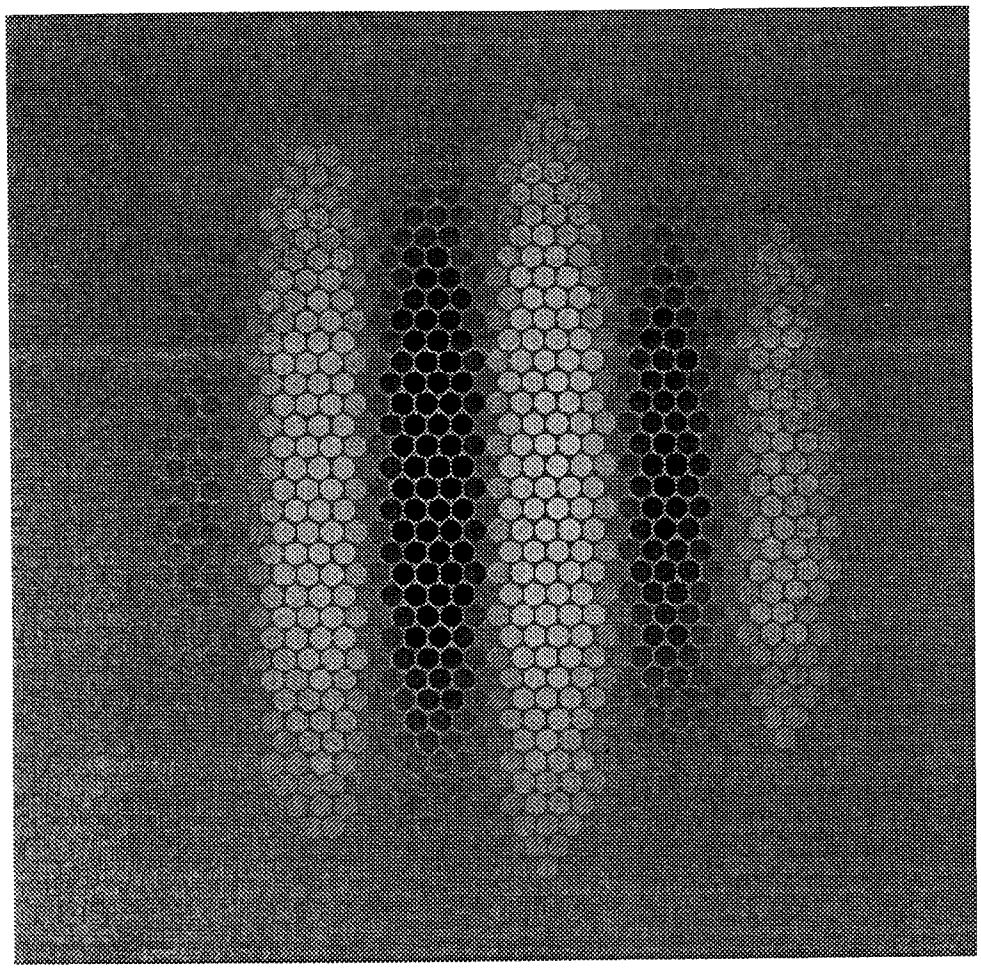

A

FIG. 6-22. Adult and infant receptive fields from Banks and Bennett (1988). Circles represent individual photoreceptors, with the gray value of each circle corresponding to the weight applied to the output of that photoreceptor. (A) Adult receptive field tuned to 10 cpd. (B) Adult receptive field tuned to 40 cpd. (C) Neonate receptive field tuned to 10 cpd; it is identical to the receptive field in (B) except that the photoreceptors are four times farther apart, making the point that the Banks and Bennett model can be thought of as a horizontal-shift model (provided it is restricted to regions of the spatial-frequency axis where square-root law holds and a linear NTF with a slope of -1 is a good approximation).

tons (by a factor of 4^2); so if square-root law holds, the NTF should be shifted upward by a factor of 4. Recall, however, that Banks and Bennett assumed at intermediate and high spatial frequencies (the only range over which they made a prediction) that the NTF is a line with slope -1 on a log-log plot. Obviously, for this NTF a horizontal shift by a factor of 4 is equivalent to a vertical shift by the same amount. This point is made another way in Figure 6-22, which shows three sample ideal weighting functions (the model's equivalent of receptive fields) from the Banks and Bennett analysis. Figure 6-22A shows the adult weighting function when the stimulus to be detected is a Gabor patch of 10 cpd. Each circle represents an individual cone, the size representing the diameter of the aperture, and the intensity representing the weight assigned to the output. Figure 6-22B shows the adult function for detecting 40 cpd and Figure 6-22C the infant function for detecting 10 cpd. Note that the infant weighting function for detecting 10 cpd is just a stretched version of the adult function for detecting 40 cpd. Thus given an implicit NTF of the sort assumed by Banks and Bennett and square-root law, the vertical-shift method of Banks and Bennett is perfectly compatible with connections being maintained between photoreceptors and higher neurons. Therefore the Wilson and Banks and Bennett analyses are equivalent on this point.

Earlier, we discussed some assumptions in Wilson's model, which to us seem questionable: the choice of data to represent the adult, the OTF, that square-root

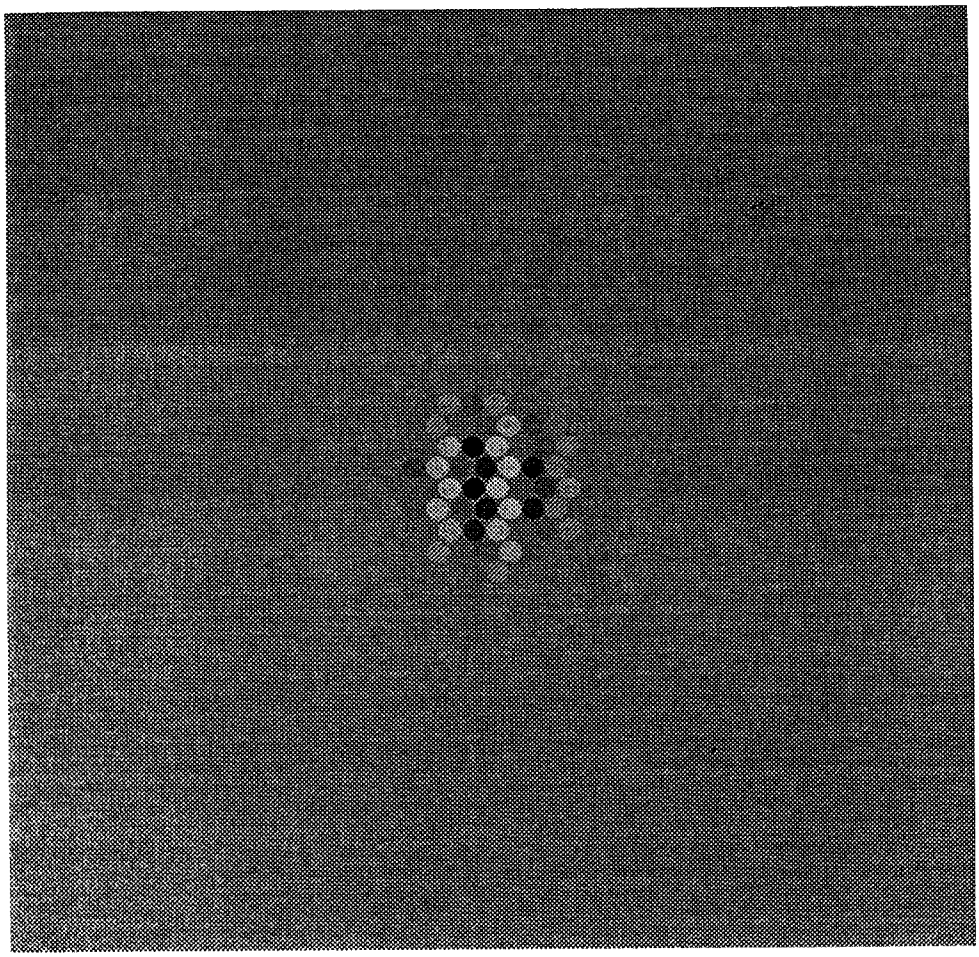

B

FIG. 6-22. (*continued*)

law holds everywhere, and the omission of the effects of changing receptor aperture. We have changed these assumptions to more reasonable ones in the next section in which we modify the Wilson model. The most significant of the assumptions is the manner in which square-root law was applied, and the difference on this point between the two analyses probably represents a difference in philosophy: Wilson's approach is simply bolder than that of Banks and Bennett. Wilson used a model of adult spatial vision as his starting point and applied the presumed effect of reduced photon catch everywhere. Banks and Bennett attempted to keep the number of assumptions to a minimum by starting with an ideal observer and tracing information losses due to immature optics and photoreceptors. They made only developmental predictions on the portion of the CSF for which square-root law holds in adults and for which the ideal observer analysis of Banks et al. (1987) predicted the shape of the adult CSF. Hence Wilson applied square-root law at all spatial frequencies, whereas Banks and Bennett applied it only to frequencies above 3 cpd.

Assumptions about the domain over which square-root law applies are crucial to modeling the factors of interest here. We know in adults that contrast sensitivity tends to follow square-root law at low to moderate photopic illuminances and medium to high spatial frequencies; and that sensitivity tends to follow Weber's law at high illuminances and low spatial frequencies (van Nes and Bouman, 1967; Kelly, 1977; Koenderink and van Doorn, 1978). Unfortunately, we do not know the range of spatial frequencies and illuminances in which square-root law holds in infants; that is, we do not know the relation between infant photopic contrast sensitivity and light level (Dannemiller and Banks, 1983; Brown et al., 1987; Fiorentini et al., 1990; Allen et al., 1992). Until such data are available, the best one can do is consider the relation in adults and assume that it is similar in infants. We have done so when creating modified versions of Wilson's model: Specifically, we assumed both square-root law and the law implied by van Nes and Bouman's data with the expectation that the correct assumption is contained within these extremes.

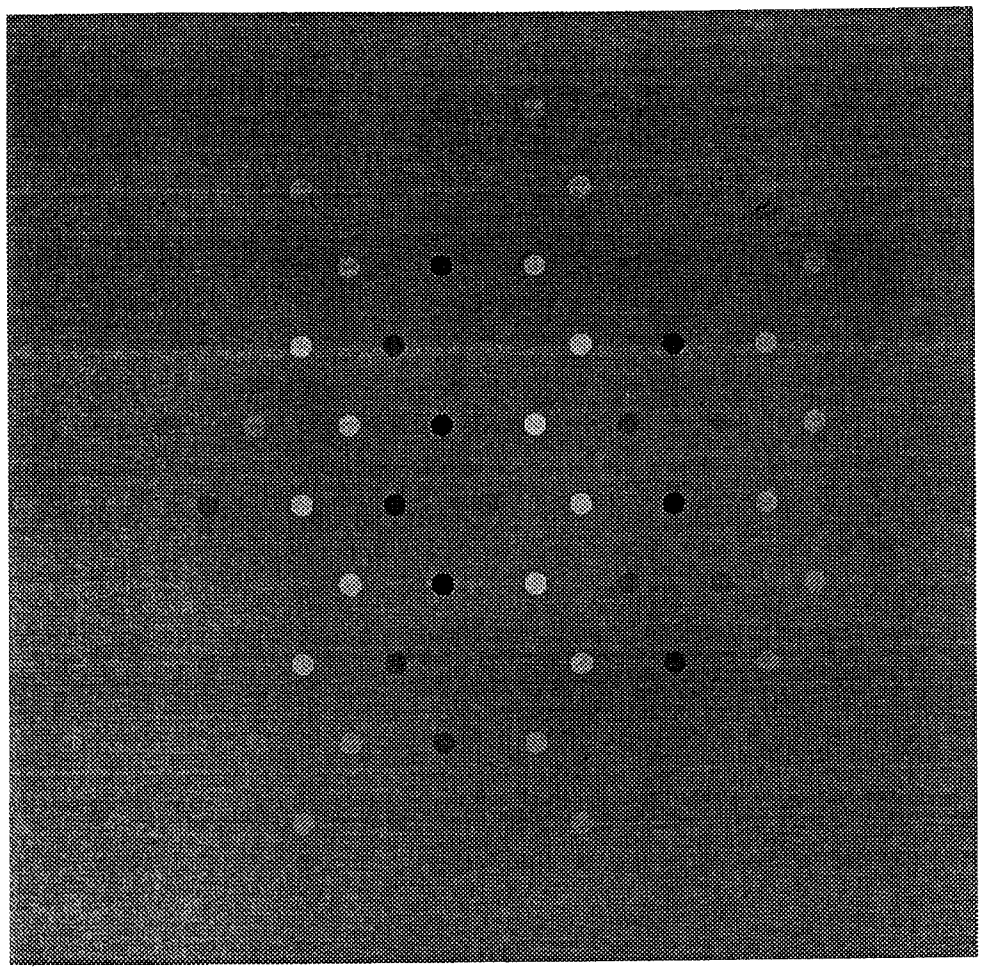

C

FIG. 6-22. (*continued*)

MODIFIED VERSION OF WILSON'S MODEL

The central concept of Wilson's model—that cone migration causes a horizontal shift of the NTF toward higher spatial frequencies with maturation—is interesting and plausible, but we questioned some of his assumptions about modeling parameters and data sets. Thus we modified his model by incorporating more plausible parameters and more representative data sets while retaining the underlying principle.

First, because we think that considering only VEP data artificially decreases the adult–neonate gap that has to be explained, we used a psychophysical CSF to represent the adult. The CSF data were collected by M.S.B., who has measured his own OTF using the technique of Santamaria et al. (1987); this consideration is important because there is considerable variation in optical quality among individuals (Howland and Howland, 1976; Artal et al., 1988). For most spatial frequencies the stimuli were sine wave gratings, but at the highest frequencies we used square waves, a maneuver that allowed us to measure more of the high-frequency limb of the CSF. Space-average luminance was 50 cd/m^2. Under these conditions, M.S.B.'s (natural) pupil diameter is 6 mm, resulting in a retinal illuminance of approximately 1400 td. Stimulus duration was 250 ms. At every spatial frequency, at least 10 grating cycles were presented. Thresholds were estimated using a 2IFC procedure and a two-down, one-up staircase. The choices of luminance, duration, and size of the stimulus reflect compromises in our attempt to make the data comparable to the conditions under which infant CSF's have been measured.

The function fit to these data is shown in Figure 6-13. This adult CSF is different in shape from the envelope of the six mechanisms in Wilson's adult model, probably reflecting the fact that M.S.B.'s optics are unusually sharp. Therefore, instead of fitting the mecha-

nisms of Wilson's adult model to these data, we applied the transformations of Wilson's developmental model directly to the adult CSF.

We used the measured OTF of the adult observer. Unfortunately, the largest pupil diameter for which we have his OTF was 4 mm, and his pupil diameter in the psychophysical experiment was 6 mm. This OTF is shown by the dashed curve in Figure 6-3 and was used to divide the adult data before executing the horizontal shift. To estimate the OTFs of the infants in the Banks and Salapatek (1978) and Norcia et al (1990) studies, we needed some idea of their pupil diameters; we used the average observer of Spring and Stiles (1948), who at Banks and Salapatek's luminance of 55 cd/m^2 had a pupil diameter of about 4.5 mm and at Norcia's luminance of 220 cd/m^2 a diameter of about 3.5 mm. Neonatal pupil diameters appear to be smaller than those of adults, but the numerical apertures are similar. Because the numerical aperture, rather than the pupil diameter per se, is the best predictor of optical quality (Gaskill, 1978), we used Campbell and Gubisch's 3.8-mm OTF to represent the infant optics for these conditions (3.8 being the closest measured value to 3.5–4.5 mm). Specifically, the 3.8-mm OTF was used to multiply the NTF after the horizontal shift. The effects due to age-related changes in the aperture transfer function [$R(u, v)$] were also incorporated, but these effects are small.

As stated above, we modeled the effect of the reduced photon catch due to the shorter outer segment (E) assuming both square-root law and the law implied by van Nes and Bouman's (1967) data. The adult-to-neonate drop in contrast sensitivity implied by square-root law is a rigid vertical shift by a factor of 3.4 (we used the number supplied by Banks and Bennett instead of that given by Wilson to simplify the comparison of the models). The change from adulthood to 15 months is smaller, a factor of 1.3. To implement the changes implied by van Nes and Bouman's data, we assumed that the effect of changes in illuminance on contrast sensitivity are similar in adults and neonates except for a fourfold shift in the frequency at which the effects occur (and a twofold shift for 15-month-olds). The changes implied by van Nes and Bouman's data are smaller than those implied by square-root law at lower spatial frequencies. Indeed, below 2 cpd there is no effect of reduced photon catch.

We also modified Wilson's assumptions about age-related changes in the receptor aperture. Wilson's representation of the effects of photoreceptor migration by a rigid horizontal shift on a log-frequency axis involves the implicit assumption that the aperture diameter does not change with age (see Chapter 32). As discussed above, the aperture width changes from 0.35 minute in the neonate to 0.67 minute at 15 months to 0.48 minute in the adult. In order to model the effect of changing

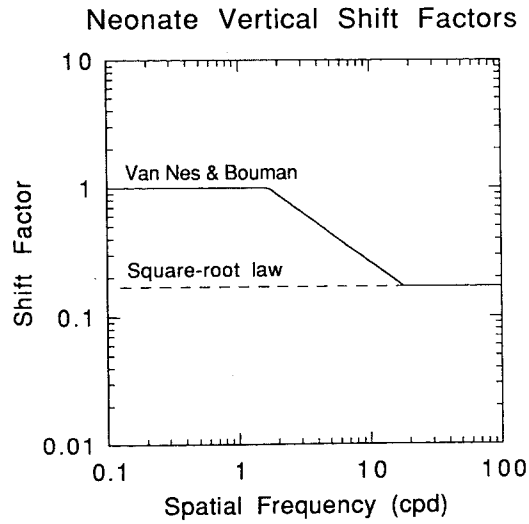

FIG. 6-23. Neonate vertical shift factors for our modification of Wilson's model (see Chapter 32) under two assumptions about how reduced photon catch affects contrast sensitivity. These figures show the combined effects of reduced outer segment length and changing photoreceptor aperture diameter. Dashed line is the shift factor assuming square-root law holds at all spatial frequencies; it is a rigid downward shift by a factor of 5.9. Solid line is the shift factor using the data of van Nes and Bouman (1967); it is smaller than the square-root law shift, and there is no shift below 2 cpd.

aperture size on photon catch, we divided the number of photons caught by the adult receptor lattice by the ratio of the adult aperture area to the infant aperture area. Again, we used the same two assumptions (square-root law and the van Nes and Bouman data) to calculate the effect of reduced quantum catch on sensitivity. Figure 6-23 shows the vertical shift factor, combining the outer segment length effect and the receptor aperture effect for the neonate under these two assumptions. The dashed lines represent square-root law and the solid lines the van Nes and Bouman data. The shift factor for 15-month-olds is much smaller than that for neonates: Assuming square-root law, it is a factor of only 1.3.

The results of all these changes on the neonate and 15-month predictions are shown in Figure 6-24. The solid curves represent the two predictions, based on the square-root law and on van Nes and Bouman's data[6]; the dotted curves represent infant VEP data, and the dashed curves are infant FPL data. In all cases, the discrepancy between predictions and data is considerable; the predicted infant sensitivities across a broad range of medium and high spatial frequencies are a log unit or more higher than the observations. We could not generate an acuity prediction because the curves

6. The predictions shown are for the Banks and Salapatek data (1978). The predictions for the Norcia et al. (1990) data are slightly higher but so similar that we did not plot them separately.

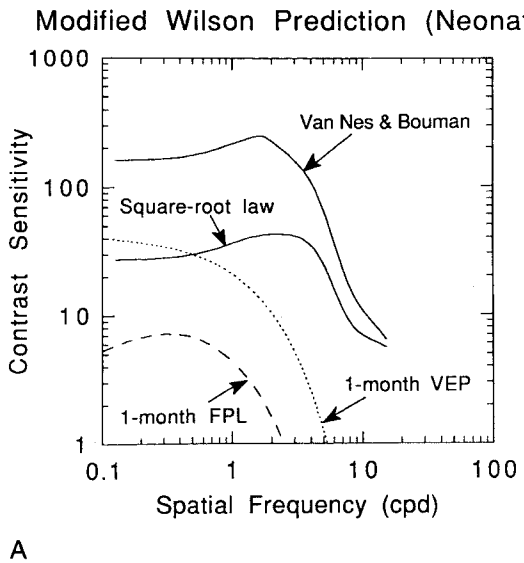

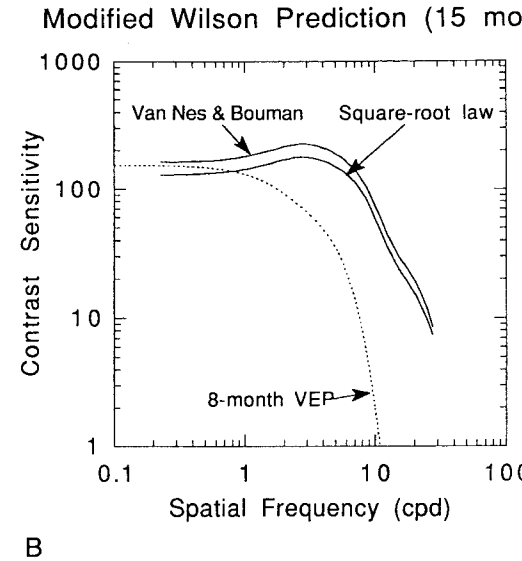

FIG. 6-24. Modified Wilson neonate (A) and 15-month (B) predictions. Solid curves are the model predictions under both square-root law and van Nes and Bouman (1967) assumptions; dotted curves represent VEP data from Norcia et al. (1990); and dashed curves represent FPL data from Banks and Salapatek (1978). The predictions approach the data only at low spatial frequencies.

never approach the horizontal axis; in order to make such a prediction, we would need adult data at sensitivities much less than 1.

Thus once more reasonable assumptions about some of the modeling parameters are employed, Wilson's model still does not account for the low contrast sensitivity of the human neonate; indeed, the prediction is farther off than before. The predictions of the original model at 15 months were similar to 8-month data, which is not the case with the modified model: predicted medium- and high-frequency sensitivities at 15 months are 0.5–1.5 log units higher than the observations at 8 months. Presumably, contrast sensitivity improves between those two ages, so perhaps data collected at 15 months will ultimately confirm the predictions.

We have applied the same assumptions about square-

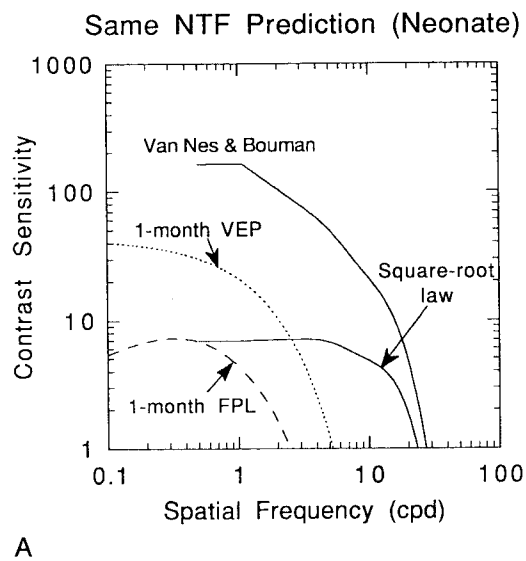

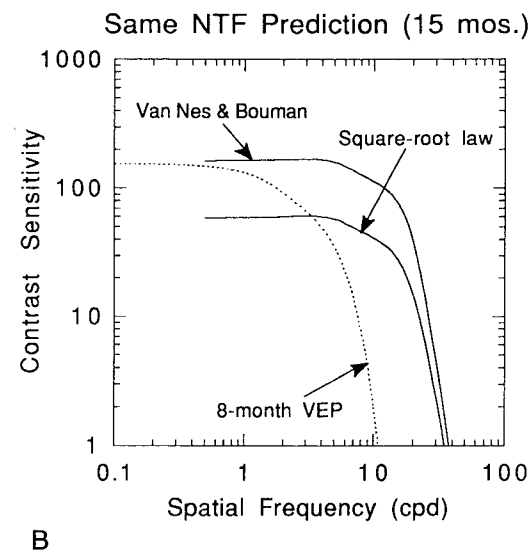

FIG. 6-25. Neonate (A) and 15-month (B) predictions under the assumption that the infant NTF is identical to that of the adult at all spatial frequencies, in contrast to laterally shifted, as in Wilson's model, or identical only at high spatial frequencies, as in the Banks and Bennett model. Unlike these two models, the neural implementation of this assumption would require that connections between receptors and higher neurons be broken and reestablished over the course of development. At each age, all receptive fields would have the same spatial profiles; adult cortical neurons would have to take inputs from many more photoreceptors. None of these assumptions comes close to explaining the observed CSFs.

root law and van Nes and Bouman's data to the Banks and Bennett model. The results are shown in Figure 6-25.

Having taken the liberty of modifying Wilson's model to include modeling parameters more similar to those used in the Banks and Bennett analysis, we should delineate any remaining differences between the two approaches. The approaches are similar in regard to how they treat changes in outer segment efficiency and eye size; so once we included the OTF and receptor apertures used by Banks and Bennett at different ages and inserted the same adult CSF as the starting point for modeling, what differences if any remain? There are three: (1) The effects of cone migration: Banks and Bennett assumed that the only direct consequence of cone migration is to change the photon catch and that that produces a vertical shift in predicted contrast sensitivity; Wilson assumed that the consequence of migration is a change in the preferred frequencies of his six channels and that that produces a horizontal shift of the NTF. (2) The shape of the NTF: Banks and Bennett implicitly assumed a constant-bandwidth NTF, whereas Wilson implicitly assumed an NTF of a different shape (at low and intermediate frequencies anyway) that was required to account for his adult CSF data. (3) The assumed domains over which square-root law applies: Banks and Bennett restricted their analyses to spatial frequencies for which that assumption has been shown to be valid in adults, and Wilson applied square-root law everywhere. Interestingly, the differing assumptions concerning cone migration have no effect on the predictions because, for the NTF implied by Banks and Bennett's analysis, their vertical shifts due to changes in cone spacing are exactly equivalent to Wilson's horizontal shifts. So the only differences are in the shapes of the NTFs and the domain over which square-root law is assumed to apply. It is important to note that on the high-frequency limb of the CSF the assumptions in regard to NTFs and square-root law are similar.

CONCLUSION

Yuodelis and Hendrickson's (1986) description of the development of foveal cones in human infants stimulated two analyses of the factors limiting spatial vision early in life. Although the analyses used essentially the same values for the factors under examination, they came to nearly opposite conclusions. Banks and Bennett (1988) concluded that these factors imposed important constraints but by themselves were insufficient to explain the poor contrast sensitivity and acuity of human neonates; they argued that immaturities among postreceptoral processes must also limit early spatial vision. Wilson (1988) (see also Chapter 32), on the other hand, concluded that these factors were nearly sufficient and, by inference, that postreceptoral processes are not a major limit to early vision.

This chapter reviewed the two analyses and showed that neither model as originally stated actually fits the observed data, although Wilson's predictions come closer. However, some of the assumptions in Wilson's model are questionable. To see the effects of these assumptions, we modified his model while retaining its main principles. We found that these modifications led to a poorer fit, particularly at intermediate to high spatial frequencies where the modified Wilson model falls a log unit short of fitting the observed data. Consequently, both sorts of analysis lead to the conclusion that optical and photoreceptor immaturities alone are insufficient to explain the low contrast sensitivity and acuity of the human infant.

A useful result of these analyses would be a quantification of the unexplained gap between infant and adult sensitivity (the sensitivity loss that cannot be explained by age-related changes in optics and receptors). This is, unfortunately, impossible at this time because we simply do not know enough about how infants' performance is affected by the level of illumination in the tasks considered here: As we showed, differing assumptions about the effect of illumination lead to widely disparate predictions. Until we know more about this subject, further progress in understanding the effects of front-end immaturities will be difficult to achieve.

Acknowledgments. The authors thank Kirk Swenson for assistance in producing the cone lattice schematics and Stanley Klein for comments on an earlier version. This research was supported by NIH grant HD-19927 to M.S.B.

REFERENCES

ABRAMOV, I., GORDON, J., HENDRICKSON, A., HAINLINE, L., DOBSON, V., AND LABOSSIERE, E. (1982). The retina of the newborn human infant. *Science* 217, 265–267.

ALLEN, D., BENNETT, P. J., AND BANKS, M. S. (1992). The effects of luminance on FPL and VEP acuity in human infants. *Vision Res.* 32, 2005–2012.

ARTAL, P., SANTAMARIA, J., AND BESCOS, J. (1988). Phase-transfer function of the human eye and its influence on point-spread function and wave aberration. *J. Opt. Soc. Am.* [*A*] 5, 1791–1795.

BACH, L., AND SEEFELDER, R. (1914). *Atlas zur Entwicklungsgeschichte des Menschlichen Auges.* Berlin: Verlag von Wilhelm Engelmann.

BANKS, M. S., AND BENNETT, P. J. (1988). Optical and photoreceptor immaturities limit the spatial and chromatic vision of human neonates. *J. Opt. Soc. Am.* [*A*] 5, 2059–2079.

BANKS, M. S., AND SALAPATEK, P. (1978). Acuity and contrast sensitivity in 1-, 2-, and 3-month-old human infants. *Invest. Ophthalmol. Vis. Sci.* 17, 361–365.

BANKS, M. S., AND SALAPATEK, P. (1983). Infant visual perception.

In M. HAITH AND J. CAMPOS (eds.). *Biology and Infancy*. New York: Wiley, pp. 435–471.

BANKS, M. S., GEISLER, W. S., AND BENNETT, P. J. (1987). The physical limits of grating visibility. *Vision Res.* 27, 1915–1924.

BARLOW, H. B. (1958). Temporal and spatial summation in human vision at different background intensities. *J. Physiol. (Lond.)* 141, 337–350.

BLAKEMORE, C., AND CAMPBELL, F. W. (1969). On the existence of neurons in the human visual system selectively sensitive to the orientation and size of retinal images. *J. Physiol. (Lond.)* 203, 237–260.

BONE, R. A., LANDRUM, J. T., FERNANDEZ, L., AND TARSIS, S. L. (1988). Analysis of macular pigment by HPLC: retinal distribution and age study. *Invest. Ophthalmol. Vis. Sci.* 29, 843–849.

BROWN, A. M. (1990). Development of visual sensitivity to light and color vision in human infants: a critical review. *Vision Res.* 30, 1159–1188.

BROWN, A. M., DOBSON, V., AND MAIER, J. (1987). Visual acuity of human infants at scotopic, mesopic, and photopic luminances. *Vision Res.* 27, 1845–1858.

CAMPBELL, F. W., AND GUBISCH, R. W. (1966). Optical quality of the human eye. *J. Physiol. (Lond.)* 186, 558–578.

CAMPBELL, F. W., AND ROBSON, J. G. (1968). Application of Fourier analysis to the visibility of gratings. *J. Physiol. (Lond.)* 197, 551–556.

COLETTA, N. J., AND ETHIRAJAN, K. (1991). Interference fringe acuity as a function of light level. *Invest. Ophthalmol. Vis. Sci.* 32 (suppl.), 699.

DANNEMILLER, J. L., AND BANKS, M. S. (1983). The development of light adaptation in human infants. *Vision Res.* 23, 599–609.

DOBSON, V., AND TELLER, D. Y. (1978). Visual acuity in human infants: a review and comparison of behavioral and electrophysiological techniques. *Vision Res.* 18, 1469–1483.

FIORENTINI, A., PIRCHIO, M., AND SPINELLI, D. (1990). Scotopic contrast sensitivity in infants evaluated by evoked potentials. *Invest. Ophthalmol. Vis. Sci.* 19, 950–955.

GASKILL, J. D. (1978). *Linear Systems, Fourier Transforms, and Optics*. New York: Wiley.

GEISLER, W. S. (1984). Physical limits of acuity and hyperacuity. *J. Opt. Soc. Am.* [*A*] 1, 775–782.

HENDRICKSON, A., AND YUODELIS, C. (1984). The morphological development of the human fovea. *Ophthalmology* 91, 603–612.

HOWLAND, B., AND HOWLAND, H. C. (1976). Subjective measurement of high-order aberations of the eye. *Science* 193, 580–582.

JACOBS, D. S., AND BLAKEMORE, C. (1988). Factors limiting the postnatal development of visual acuity in the monkey. *Vision Res.* 28, 947–958.

KELLY, D. H. (1977). Visual contrast sensitivity. *Opt. Acta (Lond.)* 24, 107–129.

KOENDERINK, J. J., AND VAN DOORN, A. J. (1978). Visual detection of spatial contrast; influence of location in the visual field, target extent and illuminance level. *Biol. Cybern.* 30, 157–167.

LARSEN, J. S. (1971). The sagittal growth of the eye. IV. Ultrasonic measurement of the axial length of the eye from birth to puberty. *Acta Ophthalmol. (Copenh.)* 49, 873–886.

MACLEOD, D. I. A., WILLIAMS, D. R., AND MAKOUS, W. (1992). A visual nonlinearity fed by single cones. *Vision Res.* 32, 347–363.

MILLER, W. H., AND BERNARD, G. D. (1983). Averaging over the foveal receptor aperture curtails aliasing. *Vision Res.* 23, 1365–1370.

NORCIA, A. M., AND TYLER, C. W. (1985). Spatial frequency sweep VEP: visual acuity during the first year of life. *Vision Res.* 25, 1399–1408.

NORCIA, A. M., TYLER, C. W., AND HAMER, R. D. (1990). Development of contrast sensitivity in the human infant. *Vision Res.* 30, 1475–1486.

ROSE, A. (1942). The relative sensitivities of television pick-up tubes, photographic film, and the human eye. *Proc. IRE* 30, 293–300.

SALAPATEK, P., AND BANKS, M. S. (1978). Infant sensory assessment: vision. In F. D. MINIFIE AND L. L. LLOYD (eds.). *Communicative and Cognitive Abilities: Early Behavioral Assessment*. Baltimore: University Park Press.

SANTAMARIA, J., ARTAL, P., AND BESCOS, J. (1987). Determination of the point-spread function of human eyes using a hybrid optical-digital method. *J. Opt. Soc. Am.* [*A*] 4, 1109–1114.

SHLAER, S. (1937). The relation between visual acuity and illumination. *J. Gen. Physiol.* 21, 165–187.

SNYDER, A. W., AND MILLER, W. H. (1977). Photoreceptor diameter and spacing for highest resolving power. *J. Opt. Soc. Am* 67, 696–698.

SPRING, K. H., AND STILES, W. S. (1948). Variation of pupil size with change in the angle at which the light stimulus strikes the retina. *Br. J. Ophthalmol* 32, 340–346.

TELLER, D. Y. (1979). The forced-choice preferential looking procedure: a psychophysical technique for use with human infants. *Infant Behav. Dev.* 2, 135–153.

VAN NES, F. L., AND BOUMAN, M. A. (1967). Spatial modulation transfer in the human eye. *J. Opt. Soc. Am.* 57, 401.

WATSON, A. (1985). The ideal observer concept as a modeling tool. In *Frontiers of Visual Science: Proceedings of the 1985 Symposium*. Washington, DC: National Academy of Sciences, pp. 32–37.

WERNER, J. S. (1982). Development of scotopic sensitivity and the absorption spectrum of the human ocular media. *J. Opt. Soc. Am.* 72, 247–258.

WILLIAMS, D. R. (1985a). Aliasing in human foveal vision. *Vision Res.* 25, 195–205.

WILLIAMS, D. R. (1985b). Visibility of interference fringes near the resolution limit. *J. Opt. Soc. Am.* [*A*] 2, 1087–1093.

WILSON, H. R. (1988). Development of spatiotemporal mechanisms in infant vision. *Vision Res.* 28, 611–628.

WILSON, H. R., MCFARLANE, D. K., AND PHILLIPS, G. C. (1983). Spatial frequency tuning of orientation selective units estimated by oblique masking. *Vision Res.* 23, 873–882.

WYSZECKI, G., AND STILES, W. S. (1982). *Color Science: Concepts and Methods, Quantitative Data and Formulae*. New York: Wiley.

YUODELIS, C., AND HENDRICKSON, A. (1986). A qualitative and quantitative analysis of the human fovea during development. *Vision Res.* 26, 847–855.